2020-09-25

Developmental Adipogenesis and Later-Life Cardiometabolic Risk in Offspring Exposed to Dams with Metabolic Dysfunction

Mikolajczak, Anna

UNIVERSITY OF CALGARY

Developmental Adipogenesis and Later-Life Cardiometabolic Risk in Offspring Exposed to Dams with Metabolic Dysfunction

by

Anna Mikolajczak

A THESIS

SUBMITTED TO THE FACULTY OF GRADUATE STUDIES

IN PARTIAL FULFILMENT OF THE REQUIREMENTS FOR THE

DEGREE OF MASTER OF SCIENCE

GRADUATE PROGRAM IN CARDIOVASCULAR AND RESPIRATORY SCIENCES

CALGARY, ALBERTA

SEPTEMBER, 2020

Abstract

Intrauterine exposure to maternal obesity and diabetes is linked to the development of obesity and other cardiovascular disease (CVD) risk factors in the offspring. The hypothesis for this study is that impaired subcutaneous adipose tissue (SAT) expandability underlies the development of CVD risk factors in offspring born to metabolically compromised pregnancies. Female mice heterozygous for leptin receptor deficiency (Het_{db}) were used as a model of maternal metabolic dysfunction. Wild type (Wt) offspring from Wt or Het_{db} pregnancies were examined as either neonates or adults fed a control diet (CD) or a high fat/fructose (HFF) diet. Aim 1 of my study was to determine the effect of a metabolically compromised pregnancy on developmental adipogenesis. Measurement of whole-body fat mass and plasma resistin revealed that fat accumulation was heightened in neonates born to the Het_{db} vs. Wt dams. Cell size distribution data confirmed the presence of larger-sized adipocytes in the inguinal SAT (iSAT) of neonates from the Het_{db} pregnancy. Oil Red O staining, Western Blot and qPCR demonstrated a higher adipogenic potential in progenitor cells isolated from neonates born to the Het_{db} pregnancy. Aim 2 of my study was to determine if SAT dysfunction is associated with CVD risk factors in offspring born to dams with metabolic dysfunction. Offspring exposed to Het_{db} pregnancy had a predisposition for developing risk factors associated with CVD in adulthood. Higher circulating free fatty acids were accompanied by impairment of insulin-stimulated inhibition of lipolysis, indicating the manifestation of adipose tissue dysfunction. The differences in distribution of adipocyte diameter observed shortly after birth persisted into adulthood in CD-fed offspring, suggesting a predisposition to hypertrophic dysfunction, the cause of insulin resistance in adipocytes. In vitro differentiation studies in isolated adipocyte progenitors revealed that the intrinsic differentiation capacity of adipocyte-derived stem cells was not the mechanism

responsible for impaired SAT function. In conclusion, intrauterine exposure to metabolic dysfunction leads to accelerated developmental adipogenesis and a later-life perturbation in lipid handling. Therefore, CVD risk may arise from SAT dysfunction programmed during the critical perinatal window of SAT development.

Keywords: Fetal programming, adipogenesis, cardiovascular disease

Preface

This thesis is original, unpublished work. Supplementary data describing the metabolic phenotype of dams and offspring were generated by Dr. Jennifer Thompson. Cell size distribution analyses for both neonates and offspring were performed by Dr. Jennifer Thompson with contributions from Dr. Nada Sallam. Stromal vascular fraction isolation, adipocyte progenitor culture, Oil Red O Staining, RNA extraction, cDNA generation, protein extraction and Western blots were all performed independently by the author, Anna Mikolajczak. Measurement of insulin and free fatty acid levels were made by the author, Anna Mikolajczak, with the guidance and assistance of Dr. Radha Singh. Breeding, genotyping and measurement of plasma resistin levels were performed by Dr. Nada Sallam. Animal protocols used for the thesis were approved by the University of Calgary Animal Care Committee (AC17-0149).

Acknowledgements

I am incredibly thankful to have conducted research in the Thompson Lab over the last 2 years. First and foremost, I would like to express my gratitude to my supervisor, Dr. Jennifer Thompson. She has been a phenomenal mentor in the lab. I have gained the skills necessary to perform laboratory techniques independently and confidently. Dr. Thompson has given me the opportunity to present my data at several conferences, including the Perinatal Biology Symposium in Snowmass, Colorado. She has gone above and beyond to establish a positive work environment and to provide me with the resources that I need to be a successful researcher. I would like to thank my committee members, Drs. Donna Slater and Carol Huang, for their continuous guidance in my project. My committee members have inspired me to seek new knowledge and their suggestions have allowed me to progress in my research. I would like to extend my warmest thanks to my fellow lab members, Dr. Nada Sallam, Dr. Radha Singh, Dr. Cini John, Sarah Easson and Emma Walsh. They have assisted me in the completion of experiments and have been a wonderful group to collaborate with. Finally, I would like to acknowledge ACHRI for selecting me as the recipient of the Graduate Scholarship. The amazing experiences that I've had in the Master's program would not have been possible without the support of all of these individuals. I am forever grateful for my graduate school journey and I'm excited to see what the future holds.

Table of Contents

List of Illustrations and Figures

List of Tables

List of Abbreviations

Adipo-IR- Adipose tissue insulin resistance

ATD- Adipose tissue dysfunction

BAT- Brown adipose tissue

BMI- Body mass index

BMP4- Bone morphogenetic protein 4

BSA- Bovine serum albumin

$CaCl_2$- Calcium chloride

CD- Control diet

C/EBPα- CCAAT/enhancer-binding protein α

C/EBPβ- CCAAT/enhancer-binding protein β

C/EBPδ- CCAAT/enhancer-binding protein δ

CVD- Cardiovascular disease

DEPC- Diethylpyrocarbonate

FABP4- Fatty acid-binding protein 4

FBS- Fetal bovine serum

FFAs- Free fatty acids

GDM- Gestational diabetes mellitus

Gd17- Gestational day 17

GLUT4- Glucose transporter type 4

HbA1c- Hemoglobin A1c

HDL- High-density lipoprotein

H&E- Hematoxylin and eosin

Het_{db}- Heterozygous for leptin receptor deficiency

HFD- High fat diet

HFF- High fat/fructose

HIF1α- Hypoxia-inducible factor 1 α

HOMA-IR- Homeostatic model assessment of insulin resistance

IFN-γ- Interferon-γ

IGF-1- Insulin-like growth factor 1

IL-6- Interleukin 6

IP- Intraperitoneal

iSAT- Inguinal SAT

JNK- c-Jun N-terminal kinase

KCl- Potassium chloride

LGA- Large-for-gestational age

LOX- Lysyl oxidase

LPL- Lipoprotein lipase

LXR- Liver X receptor

MCP-1- Monocyte chemoattractant protein-1

NaCl- Sodium chloride

Pd21- Postnatal day 21

Pen Strep- Penicillin streptomycin

PPARγ- Peroxisome proliferator-activated receptor γ

Pref-1- Preadipocyte factor-1

qPCR- Quantitative polymerase chain reaction

SAT- Subcutaneous adipose tissue

SCD1- Stearoyl-CoA desaturase 1

SREBP1- Sterol regulatory element-binding protein 1

SREBP1c- Sterol regulatory element-binding protein 1c

SVF- Stromal vascular fraction

TD-NMR- Time-domain nuclear magnetic resonance

T2DM- Type 2 diabetes mellitus

TNF-α- Tumour necrosis factor-α

VAT- Visceral adipose tissue

VLDL- Very-low-density lipoprotein

WAT- White adipose tissue

Wt- Wild type

Zfp423- Zinc finger protein 423

Chapter 1: Introduction, Rationale and Aims

Introduction

The fetal environment and disease risk throughout the lifespan

Dr. David Barker is widely recognized for introducing the theory of 'fetal origins of adult disease' or 'fetal programming' (Calkins & Devaskar, 2011) (Marciniak et al., 2017). Fetal programming is defined as developmental aberrations in the fetus, resulting from a suboptimal intrauterine environment (Marciniak et al., 2017). These developmental perturbations can have adverse consequences for the health and well-being of the offspring in the future (Marciniak et al., 2017). The first epidemiology studies revealed an association between low birth weight and chronic disease development in adulthood (De Boo & Harding, 2006). For instance, the Dutch famine of 1944-1945 was a key historical event used by researchers to explore the consequences of maternal undernutrition on the later-life health of the offspring (Roseboom, 2019). Adults born during the Dutch famine were at higher risk for obesity, glucose intolerance and other risk factors for chronic disease (Calkins & Devaskar, 2011). These studies highlighted the importance of timing of the nutritional insult in the determination of the offspring's phenotype (Calkins & Devaskar, 2011). The prominent findings of the Dutch Hunger Winter study laid the foundations for further research in the area of fetal programming (Roseboom, 2019). The association between low birth weight and later-life chronic disease was substantiated in numerous studies around the world (De Boo & Harding, 2006). Later, it was discovered that not only small babies, but babies born large-for-gestational age (LGA) are at risk for later adverse consequences (Boney, Verma, Tucker, & Vohr, 2005).

Evidence suggests that offspring born to obese or diabetic mothers have a predisposition for higher adiposity (Heslehurst et al., 2019) and cardiometabolic risk factors (Bunt, Tataranni, & Salbe, 2005) during childhood, adolescence or adulthood. Metabolic syndrome refers to a constellation of morbidities, including obesity, dyslipidemia, hypertension and insulin resistance, which instigate the pathogenesis of cardiovascular disease (CVD) (Huang, 2009). This disorder is diagnosed when three or more of the following conditions are met: increased triglycerides, elevated fasting glucose, high blood pressure, decreased high-density lipoprotein (HDL) cholesterol and obesity in the abdominal region (Alberti et al., 2009). Isomaa et al. reported that individuals, aged 35 to 70, suffering from metabolic syndrome had a 3-fold higher risk of developing coronary heart disease and stroke (Isomaa et al., 2001). In addition, mortality due to cardiovascular complications occurred in 12.0% and 2.2% of individuals with and without metabolic syndrome, respectively (Isomaa et al., 2001). Deleterious lifestyle choices, such as smoking, inadequate nutrition and a lack of exercise, can all contribute to the emergence of metabolic syndrome (K. K. Ryckman, Borowski, Parikh, & Saftlas, 2013). However, the programming of metabolic syndrome can begin as early as fetal life, suggesting that a healthy intrauterine environment is critical in maintaining health throughout the lifespan (K. K. Ryckman et al., 2013).

Relationship between maternal metabolic dysfunction and CVD risk in offspring

Maternal metabolic dysfunction, particularly obesity (Chen, Xu, & Yan, 2018) and diabetes (Ferrara, 2007), is a widespread phenomenon. Obesity is diagnosed when an individual's body mass index (BMI) exceeds 30 kg/m^2 (Müller & Geisler, 2017). According to 2013/2014 statistics, 40.4 % of women in the US were classified as obese (Flegal, Kruszon-Moran, Carroll, Fryar, & Ogden, 2016). Data from 1976 to 2014 indicates that the rate of obesity in reproductive-

aged American women (18 to 49 years) has significantly risen from 7.4% to 27.5% (Singh & DiBari, 2019). Maternal obesity heightens the risk for the development of gestational diabetes mellitus (GDM) (Chu et al., 2007). GDM occurs when glucose intolerance is first observed in the second or third trimester with no evidence of diabetes existing prior to pregnancy (American Diabetes Association, 2019). This condition has been reported in 18% of pregnant women on a global scale, ranging from 9 to 25% according to the population (Sacks et al., 2012). Time trends suggest that GDM diagnosis is increasing in women all across the world (Ovesen et al., 2018) (Lavery, Friedman, Keyes, Wright, & Ananth, 2017) (Cho et al., 2015). Maternal metabolic dysfunction is a universal issue that requires urgent attention (Chen et al., 2018) (Ferrara, 2007).

The prevalence of obesity and diabetes during pregnancy raises concern for the development of adverse perinatal and long-term outcomes in the offspring (K. K. Ryckman et al., 2013). A retrospective study using the Helsinki Birth Cohort revealed that increased maternal BMI was associated with an increased birth weight, which resulted in a greater percentage of fat in adulthood (Eriksson, Sandboge, Salonen, Kajantie, & Osmond, 2015). Risk factors for type 2 diabetes mellitus (T2DM) and CVD were assessed in 7- to 11-year-old Pima Native children born to mothers who had diabetes during pregnancy or who developed diabetes later on in life (Bunt et al., 2005). After accounting for age, sex and adiposity, children exposed to maternal hyperglycemia in utero experienced increased hemoglobin A1c (HbA1c) and systolic blood pressure, independent of genetic susceptibility (Bunt et al., 2005). A study conducted by Bayol et al. demonstrated heightened adiposity, as well as elevated levels of glucose, insulin, cholesterol and triglycerides in the circulatory system of rats born to mothers on a junk food diet (Bayol, Simbi, Bertrand, & Stickland, 2008). Offspring born to streptozotocin-induced diabetic female rats exhibited glucose intolerance, an increase in homeostatic model assessment of insulin

resistance (HOMA-IR), a decline in HOMA insulin sensitivity and impaired pancreatic β-cell function (Aref, Ahmed, Ali, & Semmler, 2013). These human (Eriksson et al., 2015) (Bunt et al., 2005) and animal (Bayol, Simbi, Bertrand, & Stickland, 2008) (Aref et al., 2013) studies highlight the detrimental complications that arise when offspring are born to metabolically compromised pregnancies.

Furthermore, intrauterine exposure to obesity (Heslehurst et al., 2019) and diabetes (Dabelea, Knowler, & Pettitt, 2000) exacerbates the likelihood of childhood obesity, an instigator for the emergence of CVD risk factors (Nadeau, Maahs, Daniels, & Eckel, 2011). The pervasiveness of global obesity in children, ages 5 to 17 years, is increasing at an alarming rate (Lobstein & Jackson-Leach, 2016). Trends suggest that by 2025, there will be a rise in obesity from 4.8% to 5.4%, corresponding to 76 million and 91 million children, respectively (Lobstein & Jackson-Leach, 2016). Childhood obesity is linked to the development of glucose intolerance, hypertension, dyslipidemia and inflammation, which lead to CVD in adult life (Nadeau et al., 2011). A Finnish study demonstrated that a higher BMI during adolescence (12 to 18 years old) was associated with increased common carotid artery intima-media thickness, an early indicator of atherosclerosis, in both men and women (33 to 39 years old) (Raitakari et al., 2003). A 2007 study used the BMI data of Danish children, aged 7 to 13, to evaluate the risk of coronary heart disease in adults over the age of 25 (Baker, Olsen, & Sørensen, 2007). The occurrence of coronary heart disease in adulthood increased with a higher BMI in boys and girls aged 7 to 13 and 10 to 13, respectively (Baker et al., 2007). The prevalence of maternal metabolic dysfunction plays a fundamental role in the rising rates of CVD risk in the offspring (Gaillard, 2015) (Marco et al., 2012).

Insulin instigates perturbed neonatal outcomes

High fetal insulin, a consequence of maternal hyperglycemia, has been identified as a major culprit for aberrations in fetal development (Kc, Shakya, & Zhang, 2015). GDM is characterized by progressive insulin resistance and impaired pancreatic β-cell function (Kenna, Olsen, Spelios, Radin, & Akirav, 2016). This disorder reaches the greatest degree of severity in the third trimester (Kenna et al., 2016) and typically resolves itself at the end of pregnancy (Kirwan et al., 2004). The development of macrosomia, a birth weight exceeding 4000 grams, can be explained by the Pedersen hypothesis (Kc et al., 2015). According to this hypothesis, maternal glucose crossing the placenta stimulates insulin production from the fetal pancreas, resulting in fetal hyperinsulinemia (Kc et al., 2015). Insulin, a key regulator of fetal growth (Fowden, 1992), increases the amount of fat and protein available to the fetus, giving rise to the macrosomic phenotype (Kc et al., 2015). Researchers conducted a study in 2009 to determine if maternal glucose and cord serum C-peptide levels were predictive of neonatal adiposity measurements, such as the sum of skin folds and body fat percentage (both > 90^{th} percentile) (HAPO Study Cooperative Research Group, 2009). Elevated levels of maternal glucose and cord serum C-peptide, an index of fetal insulin, were associated with higher adiposity in the offspring (HAPO Study Cooperative Research Group, 2009). The results of this study suggest that fetal hyperinsulinemia mediates the excessive accumulation of fetal fat in hyperglycemic pregnancies (HAPO Study Cooperative Research Group, 2009). Maternal obesity is a common co-morbidity of GDM (Chu et al., 2007). Catalano et al. performed a study in 2012 to determine if maternal GDM and obesity were related to several factors assessed in the offspring, including birth weight, body fat percentage in newborns and cord serum C-peptide (all > 90^{th} percentile) (Catalano et al., 2012). Maternal GDM and obesity had an independent and synergistic effect on perturbed neonatal outcomes (Catalano et al., 2012). Elevated triglycerides in mothers with

normal glucose tolerance have been linked to higher birth weights in the neonates, which suggests that maternal lipid levels contribute to macrosomia (Di Cianni et al., 2005). In addition to macrosomia, offspring born to GDM pregnancies can develop organomegaly, particularly an enlargement of the liver (Mirghani, Zayed, Thomas, & Agarwal, 2007) and heart (Pereira, Fonseca, McGavock, & Dolinsky, 2013). Insulin is largely responsible for abnormalities in fetal growth (HAPO Study Cooperative Research Group, 2009), but other factors such as maternal lipids can also play a role (Di Cianni et al., 2005).

Intrauterine development of the SAT and adipogenesis

Insulin is an important driver for the development of adipose tissue (Otto & Lane, 2005) (Ghaben & Scherer, 2019). Visceral adipose tissue (VAT) formation is an event that is initiated in the postnatal period in the mouse (Wang, Tao, Gupta, & Scherer, 2013). In contrast, subcutaneous adipose tissue (SAT) commitment and differentiation begins between gestational days 14 and 18, suggesting that the in utero environment is critical for the proper development of the SAT (Wang et al., 2013). The proliferation of adipocyte progenitors remains elevated at birth and begins to subsequently drop in the 2 weeks following birth (Holtrup et al., 2017). The SAT of mice is further developed during puberty, a time period corresponding to postnatal days 18 to 34 (Holtrup et al., 2017). Upon completion of puberty, the number of adipocytes in adipose depots stabilize (Holtrup et al., 2017). The developmental period is critical in establishing the adipose tissue depots in adulthood (Holtrup et al., 2017).

During development, adipocytes are created through the process of adipogenesis (Otto & Lane, 2005). Adipogenesis occurs when mesenchymal stem cells give rise to preadipocytes, which then differentiate into mature adipocytes (Otto & Lane, 2005). The intrauterine signals that stimulate fetal adipogenesis have not been identified; however fetal insulin is a likely candidate given its

potent effect on in vitro adipogenesis (Otto & Lane, 2005) and critical role in fetal growth (HAPO Study Cooperative Research Group, 2009). The process of in vitro adipogenesis becomes impaired when there is a disturbance to the constituents involved in the insulin pathway, such as PI3K, AKT1 or AKT2, mTOR and the FOXO proteins (Ghaben & Scherer, 2019). Liver X receptor (LXR) has been identified as a target of insulin in the signaling cascade, which stimulates the expression of transcription factor SREBP1c (Steffensen & Gustafsson, 2004), a critical regulator of adipogenesis (Payne et al., 2009). SREBP1c is a master regulator of lipogenic enzymes involved in lipogenesis and the formation of lipid droplets (Steffensen & Gustafsson, 2004).

Adipogenesis can be divided into two phases- determination and terminal differentiation (Urrutia, Alfonso, & Mendizabal, 2018). Mesenchymal stem cells are multipotent, indicating that they have the capacity to form new cells such as adipocytes, chondrocytes and osteocytes (Zomer, Vidane, Gonçalves, & Ambrósio, 2015). A critical determinant of cell fate is the Wnt/β-catenin pathway (Christodoulides, Lagathu, Sethi, & Vidal-Puig, 2009). This signaling cascade allows the mesenchymal stem cells to commit to the osteocyte and myocyte lineage, therefore preventing the development of preadipocytes (Christodoulides et al., 2009). The Wnt/β-catenin pathway also has the capacity to repress the differentiation of preadipocytes by inhibiting the expression of key adipogenic genes, such as CCAAT/enhancer-binding protein α (C/EBPα) and peroxisome proliferator-activated receptor γ (PPARγ) (Urrutia et al., 2018) (Christodoulides et al., 2009). In the determination stage, bone morphogenetic protein 4 (BMP4) is responsible for the conversion of mesenchymal stems cells into preadipocytes, therefore preventing commitment to other cell lines (Butterwith, Wilkie, & Clinton, 1996). Several genes are involved in the early regulation of adipogenesis through the exhibition of inhibitory or stimulatory effects (Urrutia et

al., 2018). Preadipocyte factor-1 (Pref-1), which is commonly referred to as DLK1/FA1, perpetuates the preadipocyte phenotype and inhibits adipogenesis (Urrutia et al., 2018) (Hudak & Sul, 2013). Pref-1, alongside fibronectin, initiates the ERK/MAPK pathway, which heightens Sox9 production (Hudak & Sul, 2013). Differentiation is suppressed when Sox9 attaches to the promotor of CCAAT/enhancer-binding protein β (C/EBPβ) and CCAAT/enhancer-binding protein δ (C/EBPδ), resulting in a hindered expression of C/EBPα and PPARγ (Hudak & Sul, 2013). Zinc finger protein 423 (Zfp423) is critical in establishing commitment to the adipocyte lineage (Wei et al., 2013). Preadipocytes must undergo mitotic clonal expansion prior to terminal differentiation (Q.-Q. Tang, Otto, & Lane, 2003). In the terminal differentiation stage, preadipocytes transition into mature adipocytes (Urrutia et al., 2018). C/EBPβ and C/EBPδ become activated during adipogenesis and stimulate the expression of C/EBPα and PPARγ (Urrutia et al., 2018), which have an amplifying effect on one another (Urrutia et al., 2018) (Madsen, Siersbæk, Boergesen, Nielsen, & Mandrup, 2014). Evidence suggests that BMP4 signaling is a potential mechanism used by Zfp423 to increase the expression of PPARγ (Wei et al., 2013). Sterol regulatory element-binding protein 1 (SREBP1) is also known for its pro-adipogenic function as a promotor of PPARγ (Moseti, Regassa, & Kim, 2016). C/EBPα and PPARγ induce the expression of several genes in mature adipocytes, including fatty acid-binding protein 4 (FABP4), glucose transporter type 4 (GLUT4), lipoprotein lipase (LPL), stearoyl-CoA desaturase 1 (SCD1) (Moseti et al., 2016) and perilipin (Ghaben & Scherer, 2019). Thus, terminal differentiation of mature adipocytes orchestrated by a cascade of adipogenic and lipogenic genes drives the development of SAT depots during the perinatal period (Urrutia et al., 2018).

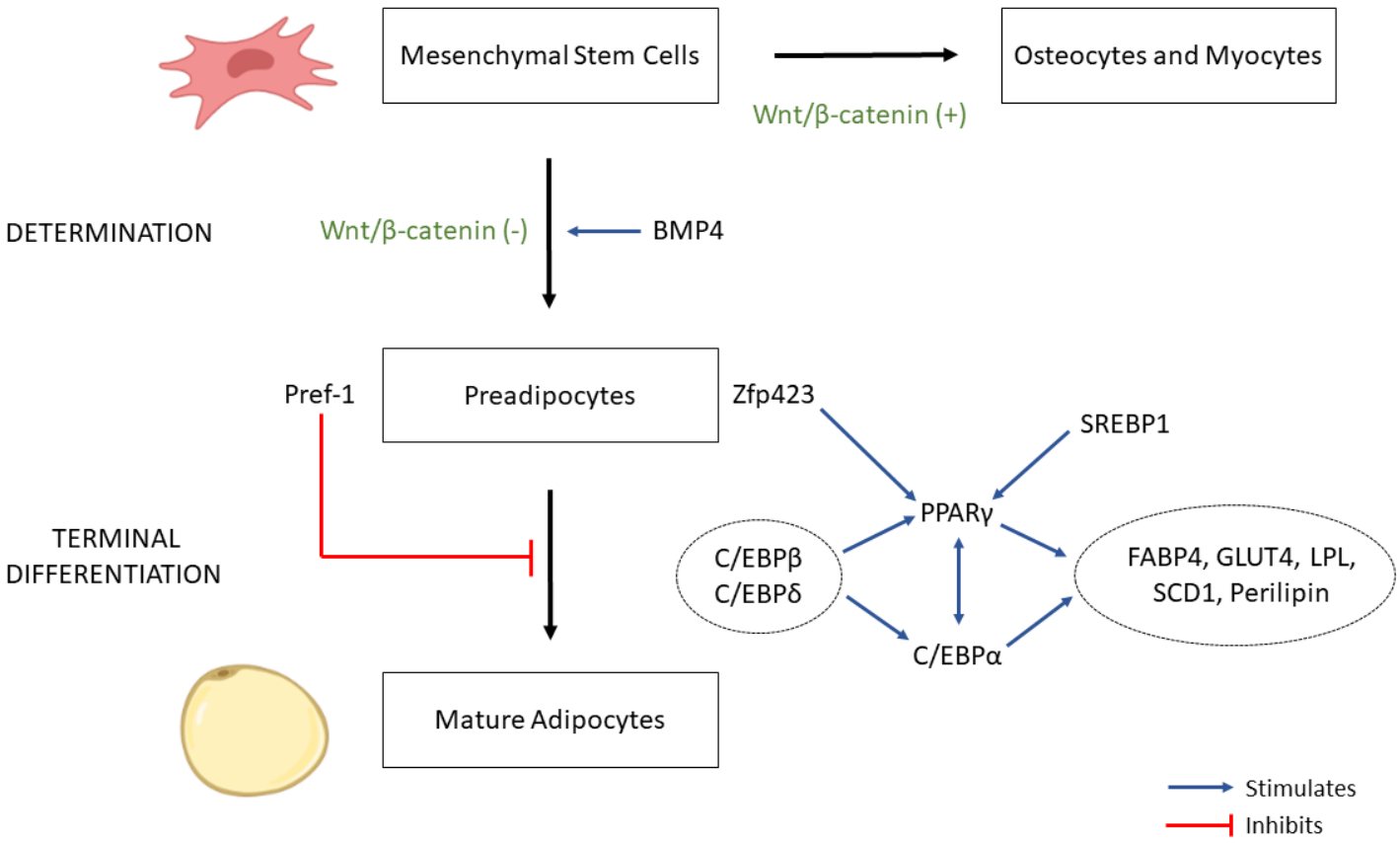

Figure 1. Schematic illustrating the process of adipogenesis. Adipogenesis occurs when mesenchymal stem cells give rise to preadipocytes, followed by differentiation into mature adipocytes. This schematic demonstrates the stimulatory and inhibitory effects of critical genes involved in the determination and terminal differentiation stages of adipogenesis. [Figure created with BioRender.com]

Function of the adipose tissue

Adipose tissue has been recognized as a potential target for the management of obesity and diabetes (Lee, Lee, & Oh, 2019). There are two main types of adipose tissue- white adipose tissue (WAT) and brown adipose tissue (BAT) (Lee et al., 2019). The lipid droplets in WAT and BAT are characterized as large unilocular and small multilocular, respectively (Lee et al., 2019). Adipose tissue contains a stromal vascular fraction (SVF), which is comprised of mesenchymal stem cells, preadipocytes, endothelial cells and macrophages (Han, Sun, Hwang, & Kim, 2015). While BAT is responsible for generating heat, energy storage and adipokine secretion are the principal functions performed by WAT (Coelho, Oliveira, & Fernandes, 2013). With regards to energy storage, lipolysis and lipogenesis are key processes in the regulation of fat metabolism (Coelho et al., 2013). During the fasting state or stress, lipolysis is initialized, resulting in the conversion of triglycerides into free fatty acids (FFAs) for utilization by other tissues (Coelho et al., 2013). Lipogenesis occurs during the feeding state, in which FFAs or carbohydrates are synthesized into triglycerides for storage in the adipose tissue (Coelho et al., 2013). In response to excess calories, the adipose tissue undergoes hyperplasia and hypertrophy (Coelho et al., 2013). Hyperplasia is an increase in the cell number, which occurs when new cells arise from a resident population of preadipocytes (Coelho et al., 2013). Hypertrophy is an increase in the size of mature adipocytes (Coelho et al., 2013). When a threshold level of hypertrophy is reached, hyperplasia is stimulated to maintain the buffering ability of adipose tissue (Ghaben & Scherer, 2019). Adequate expansion of SAT through hypertrophy and hyperplasia ensures a healthy balance of energy (Longo et al., 2019).

The adipose tissue serves an important endocrine function (Coelho et al., 2013). Cytokines, metabolites and hormones, referred to as adipokines (Choe, Huh, Hwang, Kim, & Kim, 2016),

are secreted into the bloodstream by the adipose tissue to produce an effect on target organs (Coelho et al., 2013). Leptin, resistin, adiponectin, insulin-like growth factor 1 (IGF-1), interleukin 6 (IL-6) and tumour necrosis factor-α (TNF-α) are common adipokines necessary for performing a broad range of functions (Coelho et al., 2013). For example, leptin, adiponectin and TNF-α are responsible for appetite suppression, improvement of insulin sensitivity and mediation of inflammation, respectively (Majka, Barak, & Klemm, 2011). Energy storage and adipokine secretion in WAT is pivotal in the maintenance of metabolic homeostasis throughout the body (Coelho et al., 2013).

The function of WAT can be further explored in reference to the depot location (Kwok, Lam, & Xu, 2016). The major depots of WAT are subcutaneous and visceral, which correspond to fat situated underneath the skin and surrounding vital organs, respectively (Kwok, Lam, & Xu, 2016). SAT is present in the abdominal and gluteal-femoral area, while VAT is located in the epicardial, omental and mesenteric region (Kwok et al., 2016). In comparison to the VAT, the SAT has a greater capacity for energy storage (Bjørndal, Burri, Staalesen, Skorve, & Berge, 2011) (Bays, 2014). As a result, the SAT acts as a "metabolic sink" that prevents lipid spillover into the VAT and non-adipose organs, such as the liver, heart and skeletal muscle (Bjørndal et al., 2011) (Longo et al., 2019). When compared to the SAT, the VAT plays a more active role in the metabolic process of lipolysis, therefore, the introduction of FFAs to the circulatory system is heightened by VAT (Bjørndal et al., 2011) (Majka et al., 2011). Adipokine secretion differs significantly between the two depots of adipose tissue, as observed by increased levels of leptin and adiponectin in SAT and increased levels of IL-6 in VAT (Coelho et al., 2013). A human study conducted by Fox et al. demonstrated that the link to unfavourable cardiometabolic outcomes was stronger in VAT than SAT (Fox et al., 2007). Tran et al. revealed that

transplanting SAT to the visceral cavity of a mouse resulted in a protective phenotype, which included a reduction in total fat mass, enhanced insulin sensitivity and a decrease in glucose and insulin levels (Tran, Yamamoto, Gesta, & Kahn, 2008). The subcutaneous and visceral depots in the WAT have distinct characteristics and are critical in performing a diverse range of functions (Kwok et al., 2016).

Association between SAT expansion, adipose tissue dysfunction and CVD risk

Expansion of the SAT is necessary for buffering excess energy (Longo et al., 2019). As stated by the adipose tissue expandability hypothesis, the adipose tissue has a defined capacity to expand (Virtue & Vidal-Puig, 2010). When weight gain occurs, the adipocytes increase in number and size until the limit of adipose tissue expansion is reached (Virtue & Vidal-Puig, 2010). Normal functioning adipose tissue requires adipogenesis to minimize excessive hypertrophy of existing adipocytes by dispersing the lipid accumulation to smaller, recently developed adipocytes (Ghaben & Scherer, 2019). This process is impaired in the SAT of obese individuals, as seen by the attenuated ability of the preadipocytes to differentiate (Isakson, Hammarstedt, Gustafson, & Smith, 2009). To monitor the response of the SAT to prolonged high fat diet (HFD) feeding, Wang et al. used an AdipoChaser mouse to trace mature adipocytes (Wang et al., 2013). The authors determined that HFD-induced SAT expansion occurred first by hypertrophy (Wang et al., 2013). Chatterjee et al. reported that a chronic HFD disrupted the adipogenic potential of murine cells, resulting in the formation of abnormal adipocytes incapable of handling caloric stress (Chatterjee et al., 2014). In comparison to a lean state, obese individuals have a reduced number of committed preadipocytes in the SAT, suggesting that there is a premature depletion of the preadipocyte stores and a subsequent increase in the size of existing adipocytes

(Tchoukalova, Koutsari, & Jensen, 2007). The hyperplastic and hypertrophic mechanisms of SAT expandability are critical in moderating surplus energy (Longo et al., 2019).

Recent evidence suggests that a loss of expansion capacity in the SAT is an important pathogenic event in the development of CVD risk factors (Bays, 2014). When the adipose tissue becomes inefficient in its energy buffering ability, adipose tissue dysfunction (ATD) occurs (Goossens & Blaak, 2015). ATD is characterized by abnormal adipokine secretion, hypoxia, fibrosis, inflammation and insulin resistance (Goossens & Blaak, 2015) (Sun, Tordjman, Clément, & Scherer, 2013). An abnormal secretion of adipokines is present in dysfunctional adipose tissue as demonstrated by an increase in leptin, resistin, TNF-α and IL-6, and a decrease in adiponectin (Coelho et al., 2013). Furthermore, the adipocytes of obese individuals are hypoxic as the vasculature is unable to develop at a rate that matches the growth of adipose tissue (Halberg et al., 2009). These low oxygen levels stimulate hypoxia-inducible factor 1 α (HIF1α) (Halberg et al., 2009) (Buechler, Krautbauer, & Eisinger, 2015). HIF1α targets lysyl oxidase (LOX), an enzyme responsible for cross-linking collagen I and III (Halberg et al., 2009). HIF1α promotes a fibrotic phenotype, which diminishes the flexibility of the extracellular matrix and the expansion capacity of the adipose tissue (Buechler et al., 2015). Hypoxic conditions play a significant role in the necrosis of adipocytes, resulting in the infiltration of macrophages and inflammation (Halberg et al., 2009). Inflammation is a defense mechanism used by the body to eliminate deleterious stimuli and initiate recovery (Y.-M. Park, Myers, & Vieira-Potter, 2014). Obese individuals exhibit persistent, low-grade inflammation, as demonstrated by elevated levels of TNF-α and IL-6 in the plasma (Y.-M. Park et al., 2014). In hypertrophic adipocytes, monocyte chemoattractant protein-1 (MCP-1) recruits immune cells, such as macrophages and T-lymphocytes (Y.-M. Park et al., 2014). Macrophages, specifically in the M1 activation state,

release TNF-α (Y.-M. Park et al., 2014). These M1 macrophages are necessary for the subsequent activation of T-lymphocytes, which secrete the inflammatory cytokine interferon-γ (IFN-γ) (Y.-M. Park et al., 2014). An interaction between TNF-α and IFN-γ is required for further activation of macrophages (Parameswaran & Patial, 2010). TNF-α has the capacity to turn off the insulin signaling pathway (Y.-M. Park et al., 2014). Oxidative stress, a condition in which the activity of reactive oxygen species surpasses that of antioxidants (Mlinar & Marc, 2011), increases the expression of c-Jun N-terminal kinase (JNK), an enzyme known to attenuate insulin signaling (Y.-M. Park et al., 2014). In addition to stimulating the uptake of glucose into cells, insulin has an important role in the inhibition of lipolysis in adipose tissue (Dimitriadis, Mitrou, Lambadiari, Maratou, & Raptis, 2011). When the adipose tissue becomes insulin resistant, insulin-mediated inhibition of lipolysis is impaired, causing an increase in the level of FFAs in the bloodstream (Virtue & Vidal-Puig, 2010). Furthermore, the accumulation of FFAs in the circulatory system is due to an increase in both lipogenesis and lipolysis, and a decrease in the beta-oxidation of FFAs (Saponaro, Gaggini, Carli, & Gastaldelli, 2015). A state of lipotoxicity is generated as the excess FFAs deposit in non-adipose organs, such as the muscle and liver (Virtue & Vidal-Puig, 2010), leading to systemic inflammation and insulin resistance (Coelho et al., 2013). Elevated FFAs, a risk factor for the development of CVD, are linked to several conditions, including myocardial impairments, high blood pressure and atherosclerosis (Pilz & März, 2008). Healthy expansion of the SAT is necessary to prevent ATD and the consequent development of CVD (Bays, 2014).

Study Rationale and Hypothesis

Intrauterine exposure to maternal obesity (Bayol et al., 2008) and diabetes (Bunt et al., 2005) is linked to the development of obesity and other CVD risk factors in the offspring. Recent

evidence suggests that abnormalities in SAT expansion are an important event in the pathogenesis of CVD risk factors (Bays, 2014). The SAT's ability to expand is imperative for coping with a prolonged positive energy balance (Longo et al., 2019). In accordance with the adipose tissue expandability hypothesis, the adipose tissue has a defined capacity to expand (Virtue & Vidal-Puig, 2010). The mechanisms involved in SAT expansion are hyperplasia and hypertrophy, which can be defined as increases in adipocyte number and size, respectively (Longo et al., 2019). In healthy adipose tissue, the formation of new cells through the process of adipogenesis prevents hypertrophic-induced dysfunction of existing adipocytes (Ghaben & Scherer, 2019). Therefore, the buffering capacity of the SAT can be compromised by either a reduction in the preadipocyte pool (Tchoukalova et al., 2007) or an inability for the preadipocytes to differentiate (Isakson et al., 2009). A seminal study by Graff and colleagues showed that newly formed adipocytes in adult mice arise from cells that were restricted to the adipocyte lineage before birth (Jiang, Berry, Tang, & Graff, 2014) (W. Tang et al., 2008). Therefore, the critical perinatal window of adipose tissue development (Jiang et al., 2014) (W. Tang et al., 2008) may play a significant role in later-life adipose tissue expandability. It is possible that later-life cardiometabolic risk in offspring born to pregnancies complicated by maternal obesity or GDM (Heslehurst et al., 2019) (Bunt et al., 2005) may arise from a perturbation in fetal adipogenesis. Indeed, the most common perinatal outcome of maternal metabolic disease is macrosomia, predominantly due to excess fat mass (Kc et al., 2015). Therefore, the overarching hypothesis for this study is that impaired SAT expandability due to accelerated developmental adipogenesis underlies the development of CVD risk factors in offspring born to metabolically compromised pregnancies.

Specific Aims

In order to address this hypothesis, my research project will explore the following aims:

→ Aim 1: Determine the effect of maternal metabolic dysfunction on developmental adipogenesis

→ Aim 2: Determine if adipose tissue dysfunction underlies the development of CVD risk in offspring born to dams with metabolic dysfunction

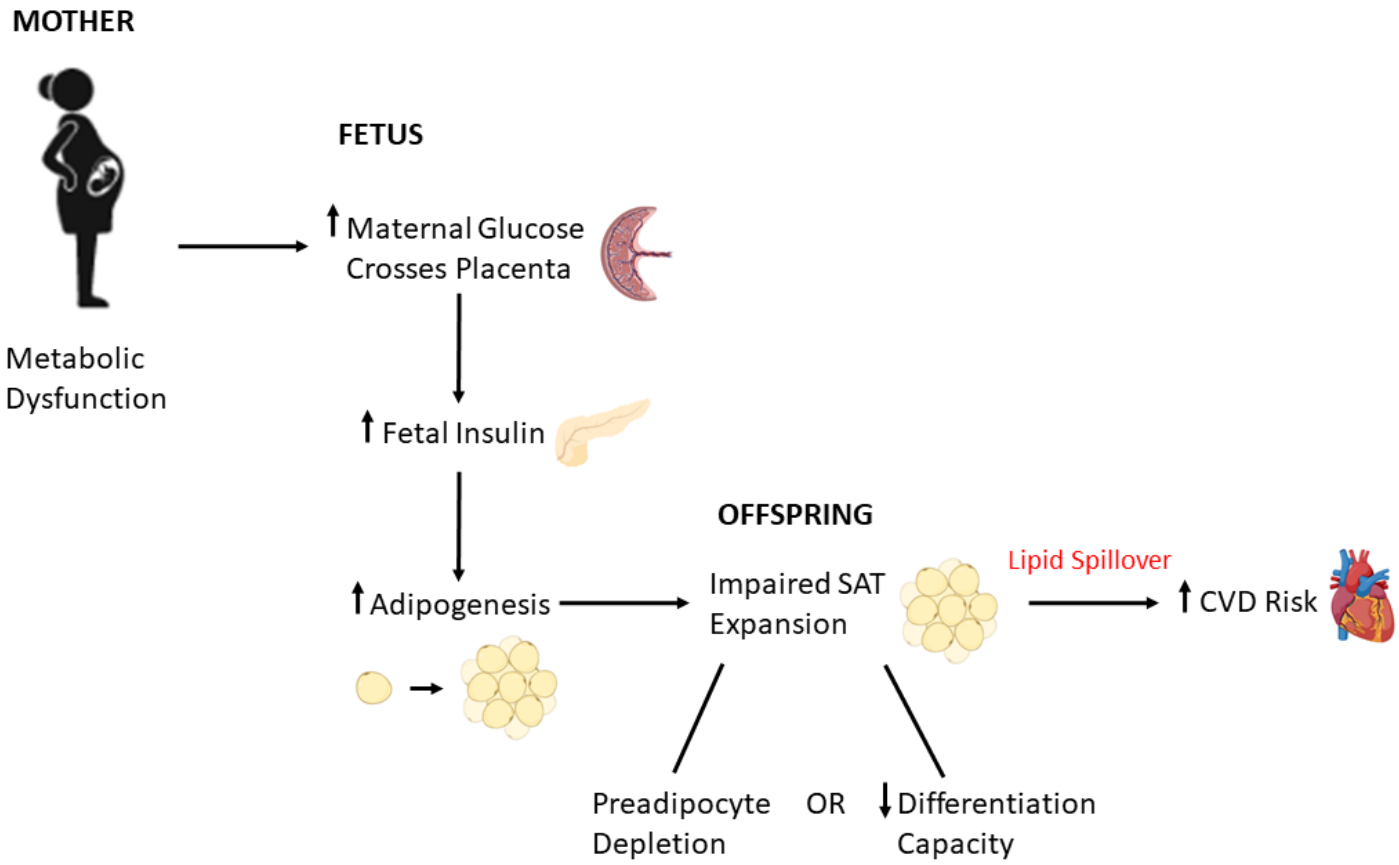

Figure 2. Graphical representation of key components in the hypothesis. In metabolically compromised pregnancies, the mother exhibits hyperglycemia. Glucose crosses the placenta and stimulates the fetal pancreas to increase the production of insulin, an inducer of adipogenesis. Accelerated fetal adipogenesis leads to a premature depletion in preadipocyte supplies or a hindered differentiation capacity later in life. Compromised SAT expandability causes lipid spillover and the subsequent development of CVD risk factors. [Figure created with BioRender.com]

Chapter 2: Models and Methods

Animal Model

Female mice homozygous for leptin receptor deficiency are severely obese and infertile (de Luca et al., 2005). Therefore, this study used heterozygotes (Het_{db}) as a model of maternal metabolic dysfunction, while age-matched C57BL/6J wild type (Wt) females were used as a control. Mice were purchased from the Jackson laboratory (strain 000697 and 000664). Het_{db} females are fertile and exhibit a phenotype reflective of global maternal metabolic dysfunction, including obesity, hyperinsulinemia, hypertriglyceridemia and hyperleptinemia. Pre-pregnancy body weight was determined in virgin Het_{db} and Wt females. Prior to pregnancy, body composition was measured using time-domain (TD) nuclear magnetic resonance (NMR) spectroscopy (Bruker). At 14 weeks of age, female mice were mated with Wt males and pregnancy confirmed with a copulatory plug. On gestational day (Gd) 17, pregnant females were sacrificed, and trunk blood collected upon decapitation. Plasma was separated by centrifugation (8000 g x 10 min) and stored for later analysis. Colorimetric assays were used to measure gestational levels of plasma insulin (ALPCO), triglycerides (ALPCO) and leptin (Abcam). In a separate cohort of pregnant females, pups were allowed to deliver spontaneously and were genotyped and weaned on postnatal day (Pd) 21. Only Wt offspring from each pregnancy were studied to isolate the programming effects of the pregnancy, independent of offspring genotype. At 7 weeks of age, offspring were fed a diet containing 45% kcal fat and 35% kcal fructose (D08040105I, Research Diets) or a control diet containing 10% kcal fat (D12450KI, Research Diets) until the day of sacrifice. The offspring were examined as either neonates or adults and males and females were analyzed separately to identify sex-specific differences.

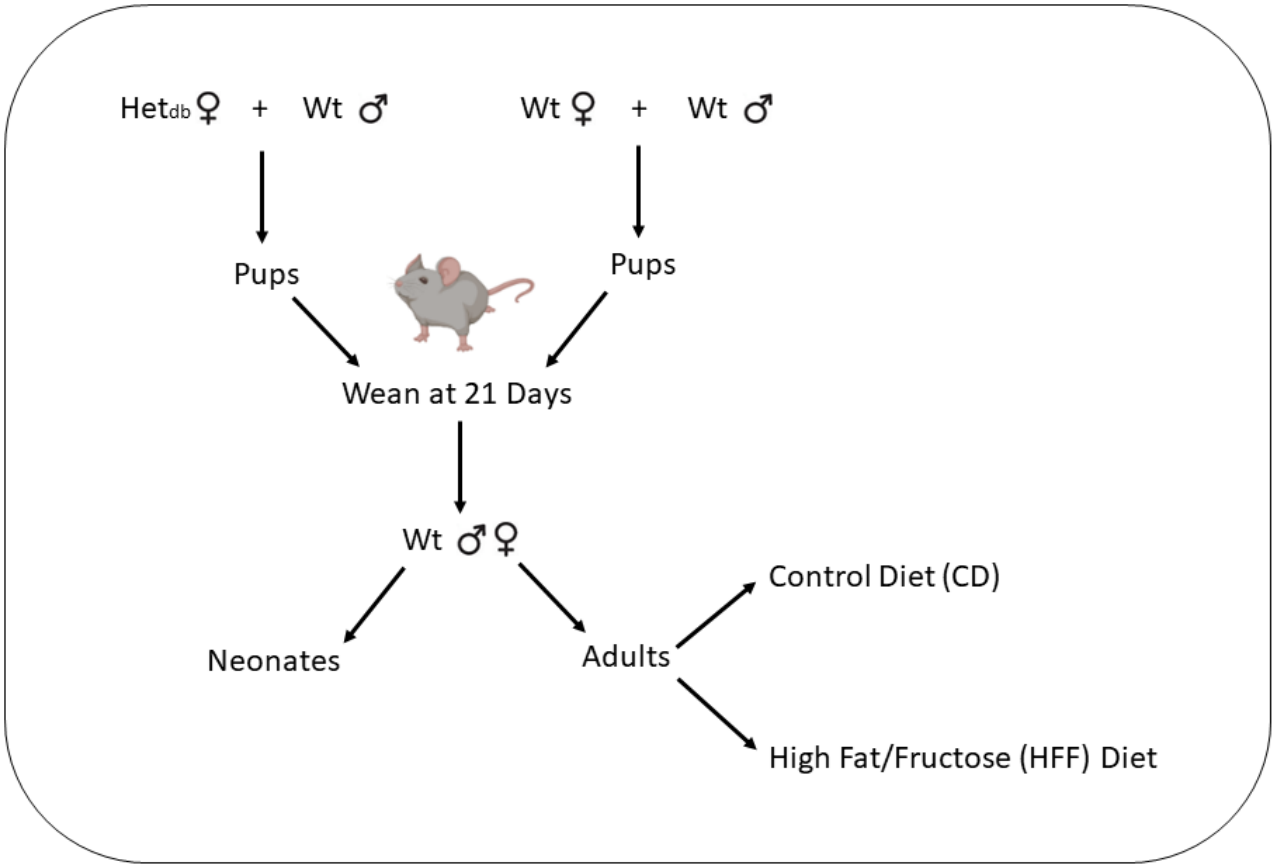

Figure 3. Experimental paradigm. 14-week old virgin Het_{db} and Wt females were mated with Wt males. The pups were weaned on Pd21. Following genotypic analysis, Wt male and female offspring were studied as either neonates or CD/HFF diet-fed adults. [Figure created with BioRender.com]

Methods

Metabolic Parameters

Time-domain nuclear magnetic resonance (TD-NMR) was used to assess whole-body fat mass. In order to determine insulin sensitivity, an insulin sensitivity test was conducted. After a 6-hour fast, an intraperitoneal (IP) injection of 0.5 IU/kg insulin was administered after measurement of baseline glucose. Following the injection, glucose levels were measured in the blood collected from the tail at time 5, 10, 15, 30, 60 and 90 minutes post-injection. Plasma free fatty acids were measured using thin layer chromatography/mass spectrometry in neonates and a Colorimetric assay (Abcam) in adults. Colorimetric assays were performed to evaluate the plasma levels of resistin (Abcam), leptin (Abcam), triglycerides (ALPCO), cholesterol (ALPCO) and insulin (ALPCO).

Resistin

Resistin levels were determined using the instructions provided by the Resistin (RETN) Mouse SimpleStep ELISA Kit. 3 µL of plasma and 117 µL of Sample Diluent NS were vortexed in a 1.5 mL Eppendorf tube. Standards 1 to 8 were prepared according to the outlined dilution scheme. In duplicates, 50 µL of each standard and sample were pipetted into the corresponding wells of the 96-well plate. 50 µL of Antibody Cocktail was subsequently added to each well. The plate was sealed and placed on a shaker at a speed of 400 rpm for 1 hour at room temperature. Following removal of the liquid, the wells were washed with 350 µL of 1X Wash Buffer PT. The plate was inverted and blotted against a clean paper towel to remove the excess liquid (the washing step was repeated 4X). 100 µL of TMB Substrate was pipetted into each well. The plate was sealed and placed on a shaker at a speed of 400 rpm for 10 minutes in a dark room. 100 µL of Stop

Solution was pipetted into each well. The plate was sealed and placed on a shaker for 1 minute to mix the contents. The absorbance values were recorded at 450 nm. Once the standard curve was constructed, the concentration of resistin was calculated for each plasma sample.

Leptin, Triglycerides and Cholesterol

Leptin, triglyceride and cholesterol levels were measured according to the manufacturer's instructions.

Free Fatty Acids

Free fatty acid levels were measured using the instructions provided by the abcam Free Fatty Acid Quantification Kit (Colorimetric/Fluorometric). Standards 1 to 6 were prepared according to the outlined dilution scheme. In duplicates, 50 µL of each standard and 5 µL of each sample were pipetted into the corresponding wells of the 96-well plate. 45 µL of Fatty Acid Assay Buffer was pipetted into the wells containing samples to make a total volume of 50 µL. 2 µL of ACS Reagent was subsequently added to each well. The plate was sealed and placed on a shaker at a speed of 197 rpm for 30 minutes at 37º C. 50 µL of Reaction Mix was prepared and pipetted into each well. In a dark room, the plate was sealed and placed on a shaker at a speed of 150 rpm for 30 minutes at 37º C. The absorbance values were recorded at 570 nm. Once the standard curve was constructed, the concentration of free fatty acids was calculated for each plasma sample.

Insulin

Insulin levels were assessed using the instructions provided by the ALPCO Mouse Insulin ELISA Kit. In duplicates, 10 µL of each standard (A, B, C, D, E, Zero Standard), control (L2 and L3) and plasma sample were pipetted into the corresponding wells of the 96-well plate. 75 µL of

Working Strength Conjugate was subsequently added to each well. The plate was sealed and placed on a shaker at a speed of 852 rpm for 2 hours at room temperature. Following removal of the liquid, the wells were washed with 250 µL of Working Strength Wash Buffer. The plate was inverted and blotted against a clean paper towel to remove the excess liquid (the washing step was repeated 9 to 10X). 100 µL of TMB Substrate was pipetted into each well. The plate was sealed and placed on a shaker at a speed of 852 rpm for 15 minutes in a dark room. 100 µL of Stop Solution was pipetted into each well. The plate was sealed and placed on a shaker at a speed of 852 rpm for 1 minute to mix the contents. The 800 TS (Biotek Instruments Inc.) plate reader was used to record the absorbance values at 450 nm. Once the standard curve was constructed, the concentration of insulin was calculated for each plasma sample.

Adipo-IR

Using the plasma free fatty acid (FFA) and insulin concentrations determined above, adipose tissue insulin resistance (Adipo-IR) was calculated. The following equation was used: Adipo-IR = FFA x insulin.

SVF Isolation, Cell Culture and Differentiation of Cells

Stromal Vascular Fraction (SVF) Isolation

HEPES buffer solution was prepared according to the following protocol: 10 mL of Fisher BioReagents 1 M HEPES buffer, 90 mL of autoclaved H_2O, 0.70 g of sodium chloride (NaCl), 0.37 g of potassium chloride (KCl), 0.09 g of dextrose, 0.0147 g of calcium chloride ($CaCl_2$) and 1.5 g of bovine serum albumin (BSA). The solution was mixed using a Fisher Scientific Isotemp magnetic stirrer. It was then filtered through a 0.22 µm Millex-GP syringe filter unit. 7 mg of Worthington Biochemical collagenase type I was added to 7 mL of the HEPES buffer solution (1

mg/1 mL). The HEPES buffer/collagenase type I solution was vortexed and filtered into a 15 mL Falcon conical tube. The following solutions were filtered into two 50 mL Falcon conical tubes: Quality Biological DPBS 1X (without Ca and Mg) and Alfa Aesar RBC lysis buffer for mouse. The inguinal SAT (iSAT) was removed from the mouse using sterile procedures and washed with filtered DPBS 4X. Autoclaved scissors were used to mince the iSAT, which was then transferred to the 15 mL conical tube. The 15 mL conical tube was inserted into a Thermo Scientific tube rotator, followed by incubation at 37^{o} C for 45 minutes. An equal volume of Cell Applications Inc. Preadipocyte Growth Medium was added to the 15 mL conical tube to stop the digestion. The solution was filtered through a 100 µm Corning cell strainer into a 50 mL conical tube. It was then transferred back into another 15 mL conical tube and centrifuged at 500 g or rcf for 10 minutes on an Eppendorf Centrifuge 5430. Without disturbing the pellet, the supernatant was removed. In order to eliminate red blood cells, 1 mL of filtered RBC lysis buffer was added to the 15 mL conical tube. The solution was pipetted up and down to break up the pellet. To stop the RBC lysis buffer, 5 mL of filtered DPBS was added and mixed inside the 15 mL conical tube. The 15 mL conical tube was centrifuged at 500 g or rcf for 10 minutes. The supernatant was removed without disturbing the SVF pellet, which contains mesenchymal stem cells, preadipocytes, endothelial cells and macrophages (Han, Sun, Hwang, & Kim, 2015). Preadipocyte Growth Medium was added to the 15 mL conical tube. Once the pellet was broken up, the solution was filtered through a 70 µm Corning cell strainer into a 50 mL conical tube. 10 mL of the solution was pipetted into a 25 cm^2 Nunc EasYFlask cell culture flask. The cell culture flask was placed inside an incubator set to 37^{o} C. PBS was prepared by diluting 100 mL of Fisher BioReagents Phosphate Buffered Saline (10X Solution) in distilled H_2O to produce a total volume of 1000 mL. After 24 hours, the cells were washed with autoclaved PBS 2X and the

Preadipocyte Growth Medium was replaced. This process was repeated every 2 to 3 days until the cells reached 100% confluency.

Passaging and Plating Cells

Once 100% confluency was reached in the flask, the adipocyte progenitors were passaged and plated. All cells were studied after the first passage because adipogenic potential declines with subsequent passages. DMEM solution with 10% FBS and 1% Pen Strep was prepared according to the following protocol: 44.5 mL of Gibco DMEM/F12 (1:1) (1X), 5 mL of HyClone fetal bovine serum (FBS) and 0.5 mL of Gibco penicillin streptomycin (Pen Strep). The solution was filtered through a 0.22 µm syringe filter unit. Preadipocyte Growth Medium was removed from the flask and the cells were washed with autoclaved PBS 1X. The cells were trypsinized in 2 mL of VWR Life Science Trypsin (0.25%) EDTA (1X). DMEM with 10% FBS and 1% Pen Strep was added to the flask, and then transferred to a 15 mL conical tube. Another 3 mL of 10% FBS and 1% Pen Strep in DMEM was added to the flask and transferred to the same 15 mL conical tube. The 15 mL conical tube was centrifuged at 220 g or rcf for 5 minutes. Without disturbing the pellet, the supernatant was removed. The desired volume of Preadipocyte Growth Medium was added to the 15 mL conical tube. The solution was pipetted up and down to break up the pellet. Appropriate dishes/plates (e.g. Corning Primaria cell culture dishes, Greiner Bio-One 6-well cell culture plates and Greiner Bio-One 12-well cell culture plates) were selected. 2 mL of the solution was pipetted into each cell culture dish. In order to evenly distribute the cells, the solution was dispensed drop by drop. The dishes were moved up, down and side-to-side, followed by placement inside the incubator at 37º C. Every 2 to 3 days, the cells were washed with autoclaved PBS 1X and the Preadipocyte Growth Medium was replaced.

Quantifying Cells

In reference to the Passaging protocol above, the remainder of the cell solution in the 15 mL conical tube was used to perform a cell count. In a PCR tube, 10 µL of the solution and 10 µL of Trypan Blue were mixed and dispensed into an Invitrogen Countess Cell Counting Chamber Slide. The slide was inserted into the Invitrogen Countess II cell counter. The total concentration and percentage of live/dead cells was recorded.

Differentiating Cells

Once the cells in the dishes/plates reached 100% confluency, also referred to as contact inhibition, there was a waiting period of 48 hours before beginning differentiation (Zhang et al., 2009). Contact inhibition is a critical period, in which the mesenchymal stem cells develop adipogenic potential (Zhang et al., 2009). At 48 hours post-contact inhibition, Cell Applications Inc. Adipocyte Differentiation Medium was added. The cells were washed with autoclaved PBS 1X and the Adipocyte Differentiation Medium was replaced every 2 to 3 days. Cells Applications Inc. Adipocyte Maintenance Medium was added on Day 5. The cells were collected and analyzed on Days 0, 2, 4 and 7 of differentiation.

Oil Red O Staining

To measure lipid droplet accumulation, Oil Red O staining was performed on Days 2, 4 and 7 of differentiation. Oil Red O stock solution was prepared according to the following protocol: 0.2 g of Sigma-Aldrich Oil Red O powder and 50 mL of Sigma Life Science 2-propanol (0.4% of the total volume is Oil Red O). The solution was mixed overnight using the Fisher Scientific Isotemp magnetic stirrer. On the following day, Whatman 1 filter paper was used to filter the stock solution. Oil Red O working solution was prepared in a 3:2 ratio of Oil Red O stock solution to

distilled H_2O (e.g. 15 mL of Oil Red O stock solution and 10 mL of distilled H_2O was added to make a total volume of 25 mL). Whatman 1 filter paper was used to filter the working solution. The cells were washed with 1 mL of PBS 2X. 1 mL of Alfa Aesar paraformaldehyde (4% in PBS) was added to each well. The 12-well plate was incubated at room temperature for 1 hour. The cells were washed with 1 mL of distilled H_2O 2X. 1 mL of 60% 2-propanol (e.g. 300 mL of 2-propanol was diluted in distilled H_2O to produce a total volume of 500 mL) was added to each well for 30 seconds. 1 mL of filtered Oil Red O working solution was added to stain the cells. The 12-well plate was placed on the Fisher Scientific platform rocker at a medium speed for 10 minutes. After removing the Oil Red O working solution, the cells were washed with 1 mL of distilled H_2O until the H_2O was clear. Distilled H_2O was kept inside the well until an image was taken with the Nikon Eclipse Ts2 microscope. Using the NIS Elements Imaging software, a picture of the cells was taken in 6 different areas of the well- top left, top right, middle left, middle right, bottom left and bottom right. Lysis buffer was prepared according to the following protocol: 2 mL of Sigma Life Science IGEPAL CA-630 and 48 mL of 2-propanol (4% of the total volume is IGEPAL CA-630). 600 µL of lysis buffer was added to each well. The plate was placed on the platform rocker at a medium speed for 10 minutes. In triplicates, 100 µL was transferred from each well in the 12-well plate to the corresponding well in a Greiner Bio-One 96-well non-binding microplate. The 96-well plate was inserted into the SpectraMax M2 plate reader. Using the SoftMax Pro 7.0.2 software, the absorbance values were recorded at 490 nm. The average absorbance of the triplicates was calculated.

RT-qPCR

RNA Extraction

RNA was extracted on Days 0, 2, 4 and 7 of differentiation using the instructions provided by the Qiagen RNeasy Mini Kit. The medium was removed from the cell culture dish or the 6-well plate. The cells were washed with 2 mL of diethylpyrocarbonate (DEPC) H_2O. In order to lyse the cells, 350 to 600 µL of Buffer RLT was added. The cells were scraped into a 1.5 mL Eppendorf tube and were subsequently vortexed. In order to homogenize the solution, a blue pestle was used, followed by a Monoject needle (23 GA, 3/4 A, 0.6 mm 19.0 mm) and syringe. The Eppendorf Centrifuge 5425 was set to 23^o C. The Eppendorf tube was centrifuged at 21330 g or rcf (maximum speed) for 3 minutes. While avoiding the debris at the bottom, the supernatant was transferred to another Eppendorf tube. An equal volume of 70% ethanol (e.g. 35 mL of 100% ethanol was diluted in DEPC H_2O to produce a total volume of 50 mL) was added to the supernatant. 700 µL of the solution was added to a spin column held within a collection tube. It was centrifuged at 8000 g or rcf for 15 seconds. The solution in the collection tube was discarded. 700 µL of Buffer RW1 was added. The spin column held within the collection tube was centrifuged at 8000 g or rcf for 15 seconds. The solution in the collection tube was discarded. 500 µL of Buffer RPE was added. It was centrifuged at 8000 g or rcf for 15 seconds. The solution in the collection tube was discarded. Another 500 µL of Buffer RPE was added. The spin column held within the collection tube was centrifuged at 8000 g or rcf for 2 minutes. The solution in the collection tube was discarded and the spin column was placed into a new collection tube. It was centrifuged at 21330 g or rcf (maximum speed) for 1 minute. The solution in the collection tube was discarded and the spin column was placed into a new Eppendorf tube. 30 µL of RNase-Free Water was added. It was centrifuged at 8000 g or rcf for 1 minute. The RNA was stored in the -80^o C freezer. RNA quantification was performed using the Implen NanoPhotometer. The concentration (ng/µL) and purity of the sample (A260/A280 and

A260/A230 ratios) was recorded. RNA integrity was checked with Tape Station at the Genomic Core.

Reverse Transcription

In order to examine gene expression in quantitative real-time PCR experiments, the extracted RNA needs to be converted into cDNA using reverse transcription. This protocol was performed with the Invitrogen High Capacity cDNA Reverse Transcription Kit. In a PCR tube, 2 µg of RNA was diluted in the appropriate volume of DEPC water. DNA was digested in DNase (Promega) and RNase OUT Recombinant Ribonuclease Inhibitor at 37° C for 30 minutes using a Bio-Rad C1000 Touch Thermal Cycler. The reaction was terminated with addition of DNase Stop Solution (Promega) and incubation for 10 minutes at 65° C, followed by placement on ice for 2 minutes. RT was performed with 10X RT Buffer, dNTP Mix, RT Random Primers, RNase OUT Recombinant Ribonuclease Inhibitor, DEPC water and MultiScribe Reverse Transcriptase using the following settings: 25° C for 10 minutes, 37° C for 120 minutes, 85° C for 5 minutes and 4° C for ∞. The cDNA was kept at 4° C until it was placed in the -20° C freezer for storage. cDNA quantification was performed using the Implen NanoPhotometer to ensure that the reaction was efficient.

Quantitative Polymerase Chain Reaction (qPCR)

Each cDNA sample was diluted in a 1.5 mL Eppendorf tube. 4 µL of the diluted cDNA sample was pipetted into the corresponding well of the 384-well plate and the plate was mixed and centrifuged. PCR was performed using SYBR Green (Applied Biosystems PowerUp SYBR Green Master Mix) on an Applied Biosystems QuantStudio 5 machine according to the following settings: 50° C for 2 minutes; 95° C for 2 minutes; 95° C for 1 second and 58.9° C for

30 seconds (X40). Three primer pairs were designed for each gene using NCBI and tested for specificity with melting curve analysis. The primer sequences are shown in Supplementary Table 1. Amplification was performed in triplicate. The expression of individual target genes was calculated relative to β-actin and expressed as fold change relative to the control group using the $2^{-\Delta\Delta Ct}$ method. Results were confirmed with a second housekeeping gene (Ribosomal protein L7, RPL7). Housekeeping genes were chosen based on their stability during in vitro differentiation.

Western Blot

Protein Extraction

Protein was extracted on Days 0, 2, 4 and 7 of differentiation. A protease and phosphatase inhibitor (Invitrogen) was added to 10 mL of Pierce RIPA buffer. The cells were washed with 1 mL of PBS 3X. 100 µL of the RIPA buffer and protease/phosphatase inhibitor mixture was added to the dish. The cells were scraped into a 1.5 mL Eppendorf tube, followed by placement in ice for 20 minutes. The sample was then vortexed and homogenized with a blue pestle. A sonication step was performed in the cells using the QSonica Sonicator (Time- 1 minute, Pulse- 5 seconds on and 10 seconds off, Amplitude- 25%). The Eppendorf tubes were centrifuged at 1500 g or rcf for 10 minutes at 4^{o} C. The supernatant was transferred to another Eppendorf tube. The protein was stored in the -80^{o} C freezer.

BCA Protein Assay

In order to determine the concentration of the extracted protein sample, a protein assay was performed using the Thermo Scientific Pierce BCA Protein Assay Kit. The previously extracted protein samples were diluted and analyzed in triplicates. The 96-well plate was read on the SpectraMax M2 plate reader. Using the SoftMax Pro 7.0.2 software, the absorbance values were

recorded at 562 nm. The average absorbance of the triplicates was calculated for each sample and protein standard. A standard curve was plotted using either the linear fit or the quadratic fit. The concentration of the sample was calculated then multiplied by the dilution factor to determine the concentration of the original protein sample.

Master Mix

A 100 µL master mix solution was prepared in a 1.5 mL Eppendorf tube according to the following protocol: 25 µL of NuPAGE LDS Buffer (4X), 10 µL of NuPAGE Reducing Agent (10X), X µL of protein sample and distilled H_2O. The protein was diluted in the master mix to produce a concentration of 1 to 2 µg/µL. The master mix solution was vortexed and kept in ice. It was then heated in the Bio-Rad Digital Dry Bath at 80^{o} C for 10 minutes, followed by vortexing.

Gel Electrophoresis

NuPAGE Bis-Tris Plus Gels (4-12%) were used for electrophoresis in an Invitrogen XCell SureLock Mini-Cell chamber with NuPAGE MES SDS Running Buffer. For proteins with a high molecular weight, NuPAGE MOPS SDS Running Buffer was used instead. 500 µL of NuPAGE Antioxidant was added to the running buffer in the inner chamber. 5 µL of the protein standard (BLUelf Prestained Protein Ladder) and the calculated volume of master mix (10 to 30 µg of protein/well) were pipetted into the desired wells using a loading tip. The gel was run at 60 V for 10 minutes, followed by 175 V for 1 hour and 15 minutes.

Transfer

A 4 L stock solution of transfer buffer (10X) was prepared, in which 121 g of UltraPure Tris and 578 g of Glycine (Electrophoresis Grade, 99+ %) were dissolved in 4000 mL of distilled H_2O.

On the day of the Western Blot, 2 L of transfer buffer (1X) was prepared according to the following protocol: 200 mL of transfer buffer stock solution (10X), 300 mL of methanol, 2 mL of 10% SDS and 1498 mL of distilled H_2O. It was stored in the -20^o C freezer until it was ready for use. The Amersham Hybond 0.45 µm PVDF membrane (6x9 cm) was activated with methanol for 15 seconds, followed by a rinse with distilled H_2O for 1 minute. The gel, PVDF membrane and 2 Bio-Rad Mini Trans-Blot Foam Pads were soaked in transfer buffer (1X) for 15 minutes. Proteins were transferred at 100 V for 2 hours in a Bio-Rad Mini Trans-Blot Cell chamber. In order to determine if the protein bands transferred from the gel to the membrane, the membrane was soaked in Sigma Ponceau S stain for 30 seconds. It was rinsed with distilled H_2O until the stain disappeared. After transfer, the membrane was blocked in 5% Bio-Rad Blotting-Grade Blocker (nonfat dry milk) in 300 mL of TBST for 1 hour at room temperature. TBST was prepared according to the following protocol: 8 g of NaCl, 0.2 g of KCl, 12.5 mL of Tris-HCl (25 mM, pH 7.5), 0.5 mL of Bio-Rad Tween-20 (0.05%) and 987 mL of distilled H_2O to produce a total volume of 1000 mL.

Primary Antibody

The expression of adipogenic markers, SREBP1 (Novus Biologicals; 1:500), FABP4 (Cell Signaling; 1:400), Adiponectin (Abcam; 1:1000), C/EBPβ (Cell Signaling; 1:500) and C/EBPα (Cell Signaling; 1:500), was examined. In order to reduce non-specific signal, the primary antibody was incubated in 1 mL of 5% milk in TBST for 1 hour in the cold room. Subsequently, the membrane was incubated in the primary antibody overnight at 4^o C. On the following day, the membrane was washed with TBST. It was placed on the platform rocker at a high speed for 10 minutes (the washing step was repeated 4X).

Secondary Antibody

The MilliporeSigma Goat anti-Rabbit (HRP) secondary antibody was used (1:5000 dilution in 5% milk in TBST). In a dish sealed with Parafilm, the membrane was covered with the secondary antibody solution. It was placed on the platform rocker at a medium speed, followed by incubation at room temperature for 1 hour. The membrane was washed with TBST. It was placed on the platform rocker at a high speed for 5 minutes (the washing step was repeated 4X).

Imaging

Depending on the strength of the signal, the Pierce ECL Western Blotting Substrate Kit or the Clarity Max ECL Western Blotting Substrate Kit were used. Equal volumes of the 2 reagents provided (Luminol/Enhancer and Peroxide) were added to the conical tube (e.g. 0.5 mL and 0.5 mL), followed by vortexing. Using a pipette, the reagent solution was applied evenly over the membrane (this was repeated several times). The membrane was placed inside a plastic sleeve, which was then positioned on the tray in the Invitrogen iBright 1500 machine. The density of the band was calculated using Volume/Area. The expression of the desired protein was determined relative to GAPDH.

Stripping the Membrane

Stripping buffer was prepared according to the following protocol: 12.5 mL of Stacking Gel Buffer (Tris HCl, 0.5 M, pH 6.8), 20 mL of 10% SDS, 67.5 mL of distilled H_2O and 800 µL of 2-mercaptoethanol. The stripping buffer was mixed in a container sealed with Parafilm, followed by incubation at 37^{o} C for 20 to 25 minutes. In the dish containing the membrane, TBST was removed and the stripping buffer was added (enough to cover the membrane). The dish was sealed with Parafilm, followed by incubation at 37^{o} C for 45 minutes. The stripping buffer was

removed. Distilled H_2O was used to rinse the membrane 4-5X. The membrane was then rinsed with TBST. It was placed on the platform rocker at a high speed for 5 minutes (the washing step was repeated 6X). The membrane was blocked with 5 % milk in TBST for 1 hour. The primary and secondary antibodies were added as described above.

Cell Size Distribution

Paraffin-embedded SAT slides were stained with hematoxylin and eosin (H&E). For each slide, 5 to 7 images were captured and subsequently analyzed using the Adiposoft (ImageJ) software. The software determines the diameter of all adipocytes in the field of view. After exclusion of artifact, the frequency of the following adipocyte diameters was determined for each view: 10, 20, 30, 40, 50, 60, 70, 80, 90, 100, 110, 120 and 130 µm. The average frequency of adipocyte diameters was calculated for all of the images captured on a slide.

Statistical Analysis

The data was expressed as mean ± SEM. The sample size was denoted as n. Statistical analyses were conducted in the GraphPad Prism 7 software. An unpaired Student's t-test was used in the neonatal data to compare the Wt vs. Het_{db} pregnancy. In the adult data, a two-way ANOVA followed by Sidak's Multiple Comparisons test was utilized to compare the Wt vs. Het_{db} pregnancy and the CD vs. HFF diet. A p-value < 0.05 was considered to be statistically significant. P-values less than 0.05, 0.01, 0.001 and 0.0001 were represented by *, **, *** and ****, respectively.

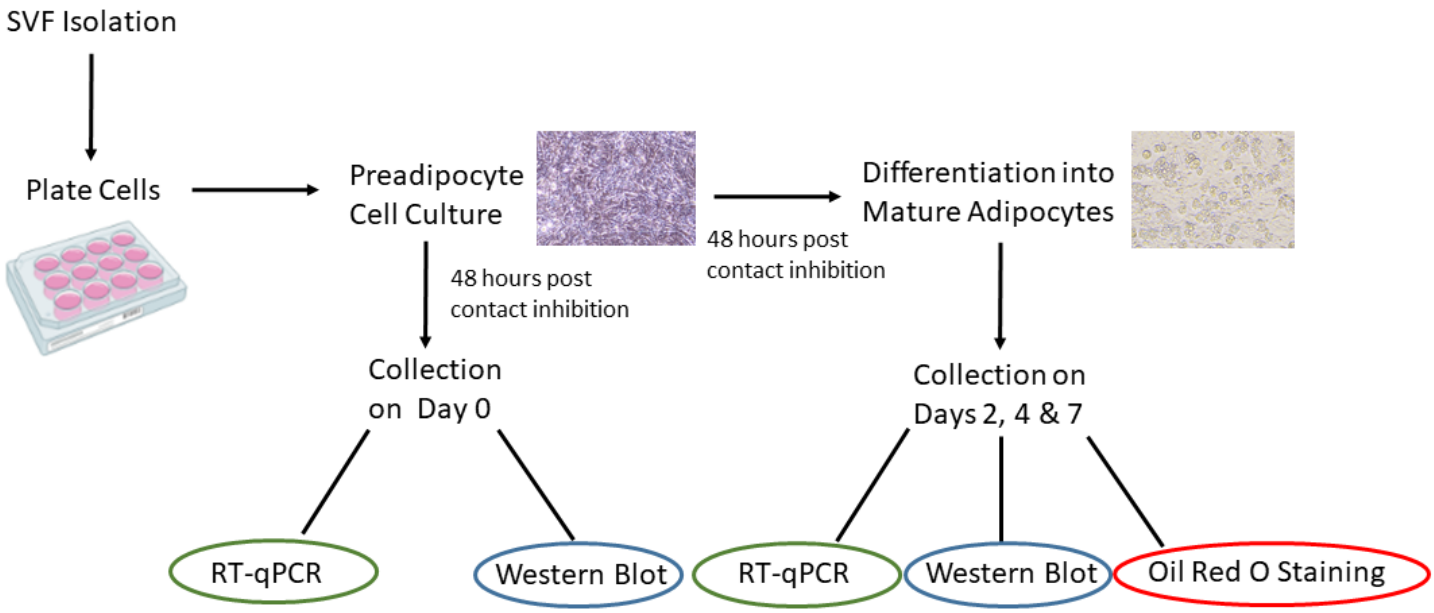

Figure 4. In vitro adipogenesis in isolated adipocyte progenitor cells. The SVF was isolated from the iSAT of a mouse. The cells were cultured and differentiated 48 hours post contact inhibition. Adipogenic potential was assessed by measuring the expression of adipogenic markers (RT-qPCR and Western Blot) and the accumulation of lipid droplets (Oil Red O Staining). [Figure created with BioRender.com]

Chapter 3: Results

Female mice heterozygous for leptin receptor deficiency exhibit characteristics of metabolic dysfunction

Pre-pregnancy body weight was 1.3-fold higher in 14-week old Het_{db} vs. Wt females (Supplementary Figure 1A). Prior to pregnancy, body composition was analyzed using nuclear magnetic resonance (NMR) spectroscopy. In comparison to Wt females, Het_{db} females had a 2.4-fold increase in whole-body fat mass (Supplementary Figure 1B) and a 13% decrease in lean body mass (Supplementary Figure 1C). Colorimetric assays revealed that plasma insulin (Supplementary Figure 1D), triglyceride (Supplementary Figure 1E) and leptin (Supplementary Figure 1F) levels were elevated in pregnant Het_{db} vs. Wt females on gestational day 17 (Gd17).

→ Aim 1: Determine the effect of maternal metabolic dysfunction on developmental adipogenesis

Accelerated developmental adipogenesis in neonates exposed to metabolic dysfunction

The development of the SAT begins in late gestation, suggesting that the intrauterine environment plays a critical role in later-life adiposity and adipose tissue function (Wang et al., 2013). NMR spectroscopy revealed that 3-week old Wt male and female neonates born to the Het_{db} pregnancy had a 32% and 33% higher whole-body fat mass, respectively (Figure 5A). There was no difference in litter size. A linear regression showed that higher whole-body fat mass was independent of litter size (data not shown). Neonates exposed to the Het_{db} dam had elevated levels of total free fatty acids (FFAs), which were positively correlated with whole-body fat mass (Figure 5B). This data shows that Het_{db} pregnancy reproduces the excessive accumulation of fetal fat mass characteristic of infants born to obese or GDM mothers (Kc et al.,

2015). Resistin, an adipokine released by mature adipocytes (H. K. Park, Kwak, Kim, & Ahima, 2017), was measured in the plasma of neonates. No differences were observed in the males, however, female neonates from the Het_{db} pregnancy exhibited a 1.7-fold increase in resistin levels (Figure 5C). There was a shift in the cell size distribution from smaller adipocytes in the iSAT of neonates born to the Wt dam to larger adipocytes in the iSAT of neonates born to the Het_{db} dam (Figure 6A). In sections of iSAT from neonates born to Wt pregnancies, there was a greater number of multilocular cells, which represent newly committed preadipocytes (Figure 6B). This finding suggests that intrauterine exposure to Het_{db} pregnancy accelerates the maturation of adipocytes in the iSAT. To determine if this premature adipocyte maturation was due to a higher adipogenic potential, differentiation was induced in adipose tissue-derived stem cells isolated from the iSAT of Wt neonates born to Wt or Het_{db} dams. Higher lipid droplet accumulation was present on Day 2 (Figure 7A) and Day 4 (Figure 7A,B) of differentiation in stem cells isolated from the neonatal iSAT of males born to the Het_{db} dam, as determined by Oil Red O staining. In male neonates from the Het_{db} pregnancy, Western Blot experiments demonstrated that mediators of adipogenesis, FABP4 and SREBP1, were increased on Day 2 of differentiation in stem cells isolated from the iSAT (Figure 8A,B). Het_{db} pregnancy was associated with a greater mRNA expression of adipogenic genes in stem cells isolated from the neonatal iSAT of males, as determined by qPCR (Figure 9). The results revealed an increased expression of Zfp423 in undifferentiated stem cells (Figure 9B), and an increased expression of Zfp423, SREBP1, C/EBPβ and mTOR in Day 2 stem cells (Figure 9A).

→ Aim 2: Determine if adipose tissue dysfunction underlies the development of CVD risk in offspring born to dams with metabolic dysfunction

Maternal metabolic dysfunction programs the development of CVD risk factors in offspring

12-week old Wt male and female offspring from the Het_{db} pregnancy had a 69% and 20% higher whole-body fat mass, respectively, as measured by NMR (Supplementary Figure 2A). Plasma triglycerides (Supplementary Figure 2B) and cholesterol (Supplementary Figure 2C) were elevated in 6-month old female adult offspring born to Het_{db} dams, in comparison to females born to the Wt dam. Following an intraperitoneal (IP) injection of insulin, the fall in glucose levels was blunted in 12-week old male offspring from the Het_{db} pregnancy, suggesting impaired insulin sensitivity (Supplementary Figure 2D). Insulin sensitivity differences were not present in female offspring fed a chow diet (data not shown).

Lipid spillover accompanies CVD risk factors in exposed offspring

Once the defined limit of SAT expansion is reached, the adipocytes become insulin resistant (Virtue & Vidal-Puig, 2010). In normal adipocytes, insulin inhibits lipolysis (Virtue & Vidal-Puig, 2010). Insulin resistant adipocytes lose this insulin-mediated inhibition, causing an increase in lipolysis and the subsequent spillover of lipids (Virtue & Vidal-Puig, 2010). In 22-week old male adults fed a CD, FFAs were elevated in offspring from the Het_{db} pregnancy (Figure 10A). The HFF diet increased FFA levels in offspring born to the Wt dam, with no further increase in offspring born to the Het_{db} dam (Figure 10A). The HFF diet increased insulin levels in male offspring from both the Wt and Het_{db} pregnancies, with a significant rise in insulin in offspring born to Het_{db} vs. Wt dams with HFF feeding (Figure 10B). In contrast, HFF feeding had no effect on FFAs (Figure 10A) or insulin (Figure 10B) in female offspring born to normal pregnancies. Females born to the Het_{db} vs. Wt pregnancy exhibited an increase in insulin when fed an HFF diet (Figure 10B). Adipo-IR is an index of insulin resistance in the adipose tissue, which is calculated by FFAs x insulin. Exposure to the HFF diet was associated with a higher Adipo-IR in male adults born to both pregnancies (Figure 10C). Female adults from the Het_{db} dam

demonstrated an increase in Adipo-IR following the consumption of an HFF diet (Figure 10C). In addition, Adipo-IR was higher in HFF diet-fed female offspring born to the Het_{db} vs. Wt pregnancy (Figure 10C).

Excess adipocyte hypertrophy is not due to an intrinsic impairment in adipogenic potential

The recruitment of new adipocytes from an existing population of preadipocytes is necessary to prevent hypertrophic-induced dysfunction of mature adipocytes and consequent lipid spillover into the bloodstream (Longo et al., 2019). The buffering capacity of the SAT can become compromised due to 1) a reduction in the preadipocyte pool (Tchoukalova et al., 2007) or 2) an inability for the preadipocytes to differentiate (Isakson et al., 2009). The preadipocyte pool that gives rise to new adipocytes in adulthood derives from cells that were committed in utero (Jiang et al., 2014) (W. Tang et al., 2008). In 12-week old Wt adults fed a CD, there was a lower frequency of smaller-sized adipocytes and an increase in the number of larger-sized adipocytes in the iSAT when exposed to the Het_{db} pregnancy (Figure 11A). The HFF diet led to an even greater reduction in smaller-sized adipocytes and a rise in larger-sized adipocytes, which eliminated adipocyte diameter differences in offspring born to Wt and Het_{db} dams (Figure 11B). In response to excess calories, adipocytes in the iSAT were able to enlarge by 85% and 22% in adult offspring from Wt and Het_{db} pregnancies, respectively, suggesting that the Het_{db} adipocytes were hypertrophic prior to HFF diet feeding (Figure 11C). In 22-week old male and female offspring, the differentiation capacity of isolated stem cells present in the SVF of adult iSAT was not altered by the type of pregnancy or diet (Figure 12). Therefore, there is no evidence to suggest that the intrinsic ability of adipose-derived stem cells to differentiate is hindered in adult offspring born to the Het_{db} dam.

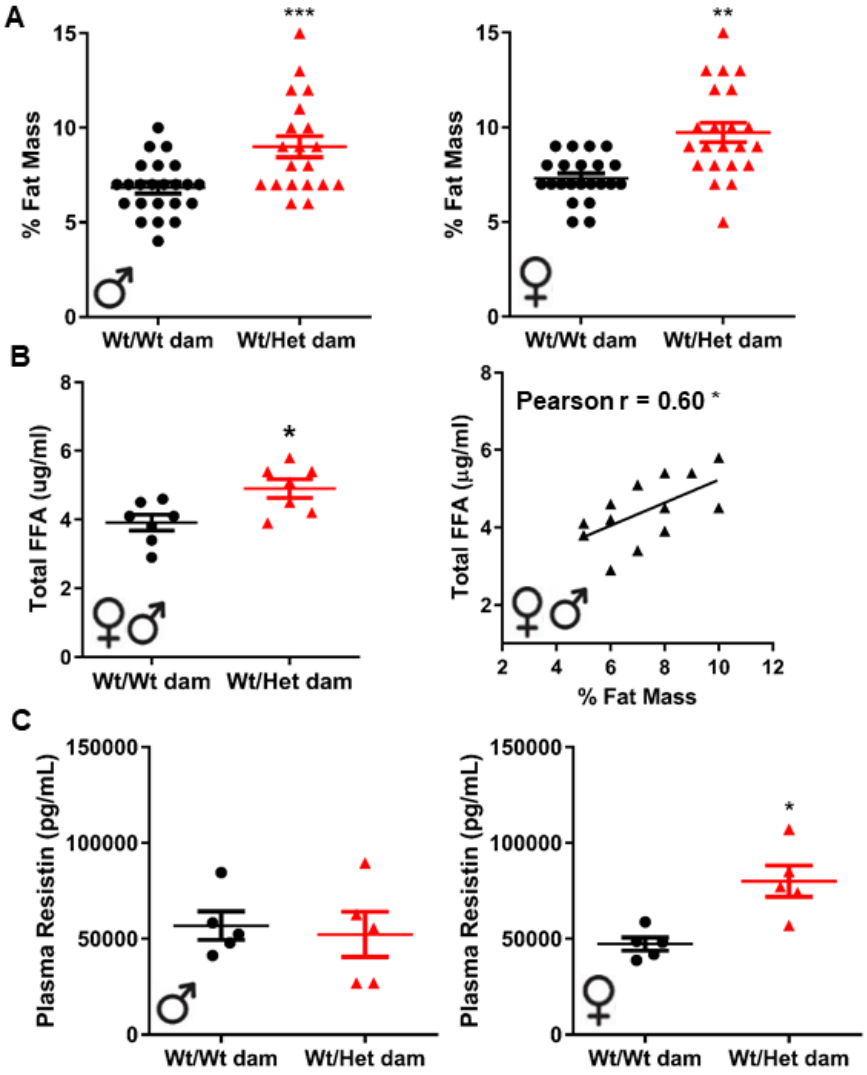

Figure 5. Fat accumulation is heightened in neonates born to dams with metabolic dysfunction. A TD-NMR whole-body composition analyzer was used to assess percent fat mass (A) in male and female neonates at the age of 3 weeks (data shown includes all offspring from 8-12 pregnancies/group). Total plasma free fatty acids (FFAs) were quantified (n = 7 pregnancies/group) and the correlation to neonatal adiposity was determined (B). The levels of resistin (C) were measured in the plasma of neonates using an ELISA (n = 5 pregnancies/group). * $p < 0.05$ Wt neonates born to Wt dams (Wt/Wt dam) vs. Wt neonates born to Het_{db} dams (Wt/Het dam). Student's t-test for A, B and C; Pearson correlation for B. [A and B were generated by Dr. Jennifer Thompson; C was generated by Dr. Nada Sallam]

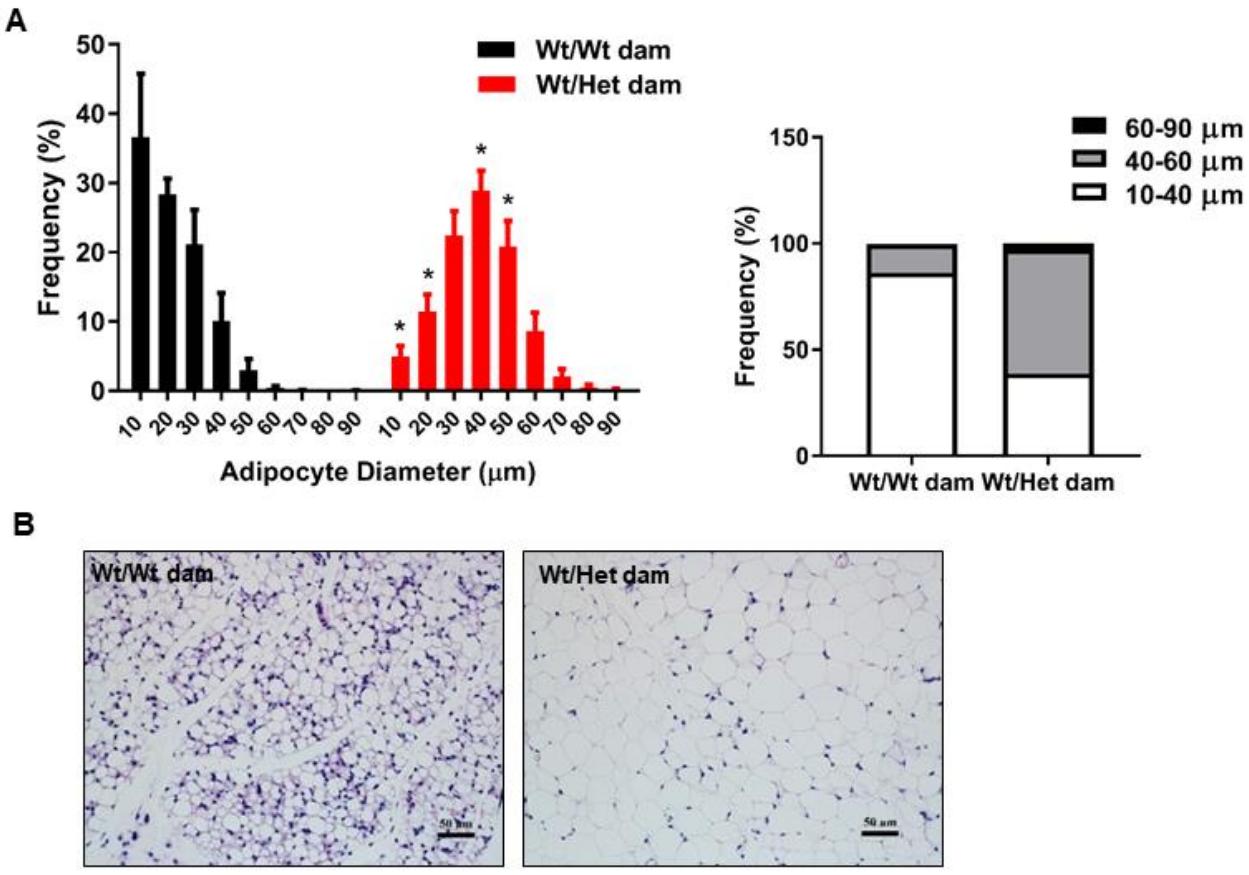

Figure 6. Adipocyte maturation is accelerated in neonates exposed to metabolic dysfunction in utero. Adiposoft (ImageJ) software was utilized to calculate the cell size distribution (A) of neonatal iSAT sections stained with H&E. Representative images of neonatal iSAT sections (B) were captured. Male and female neonates from 3 pregnancies were included for each group. * $p < 0.05$ Wt neonates born to Wt dams (Wt/Wt dam) vs. Wt neonates born to Het_{db} dams (Wt/Het dam). Data were analyzed by Two-way ANOVA followed by Sidak's Multiple Comparisons test. [Data was generated by Dr. Jennifer Thompson]

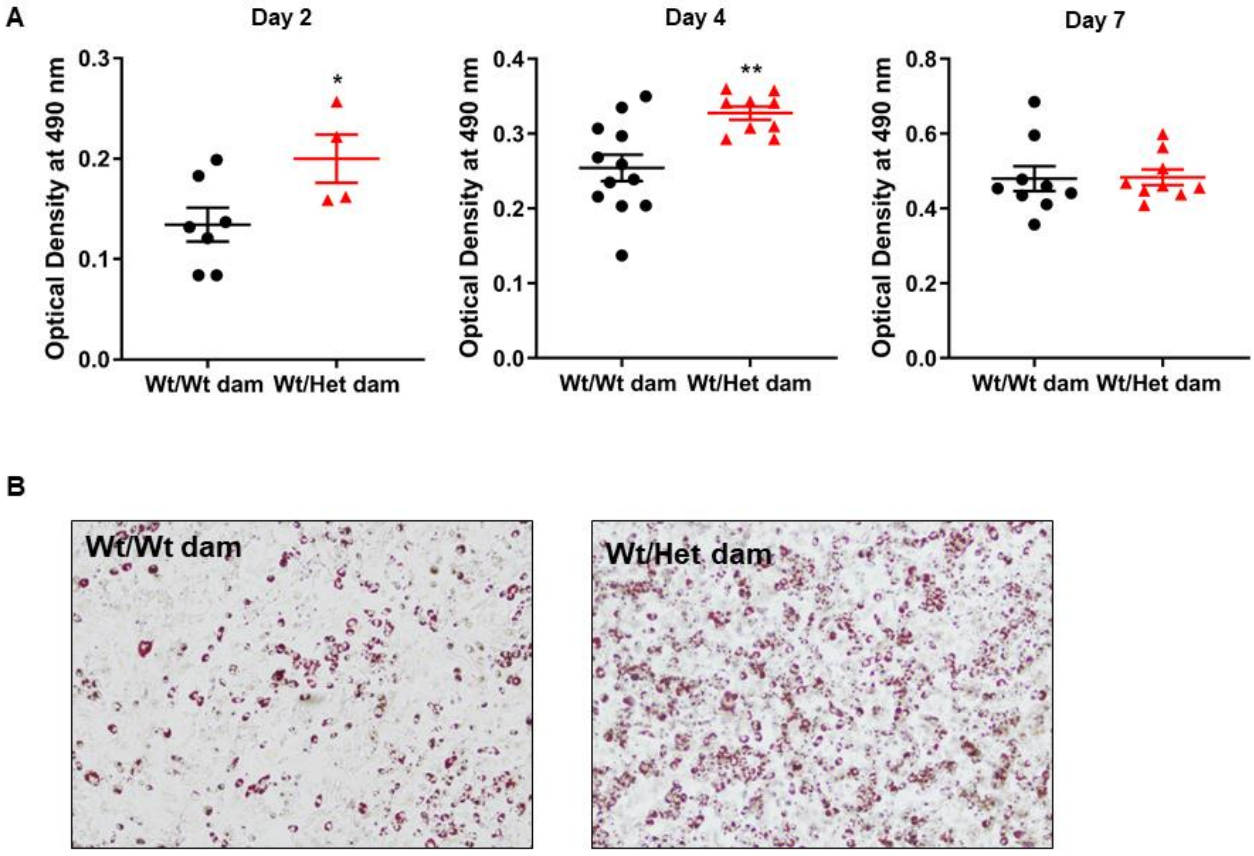

Figure 7. Higher adipogenic potential in progenitor cells isolated from neonates exposed to an adverse metabolic in utero environment. Oil Red O staining was performed on differentiated progenitors isolated from the SVF of iSAT in male neonates. Lipid droplet accumulation was quantified by optical density on Days 2, 4 and 7 of differentiation (A). Representative images were captured on Day 4 of differentiation (B). n = 3-12 pregnancies/group. * $p < 0.05$ Wt neonates born to Wt dams (Wt/Wt dam) vs. Wt neonates born to Het_{db} dams (Wt/Het dam). Significant differences were determined by Student's t-test.

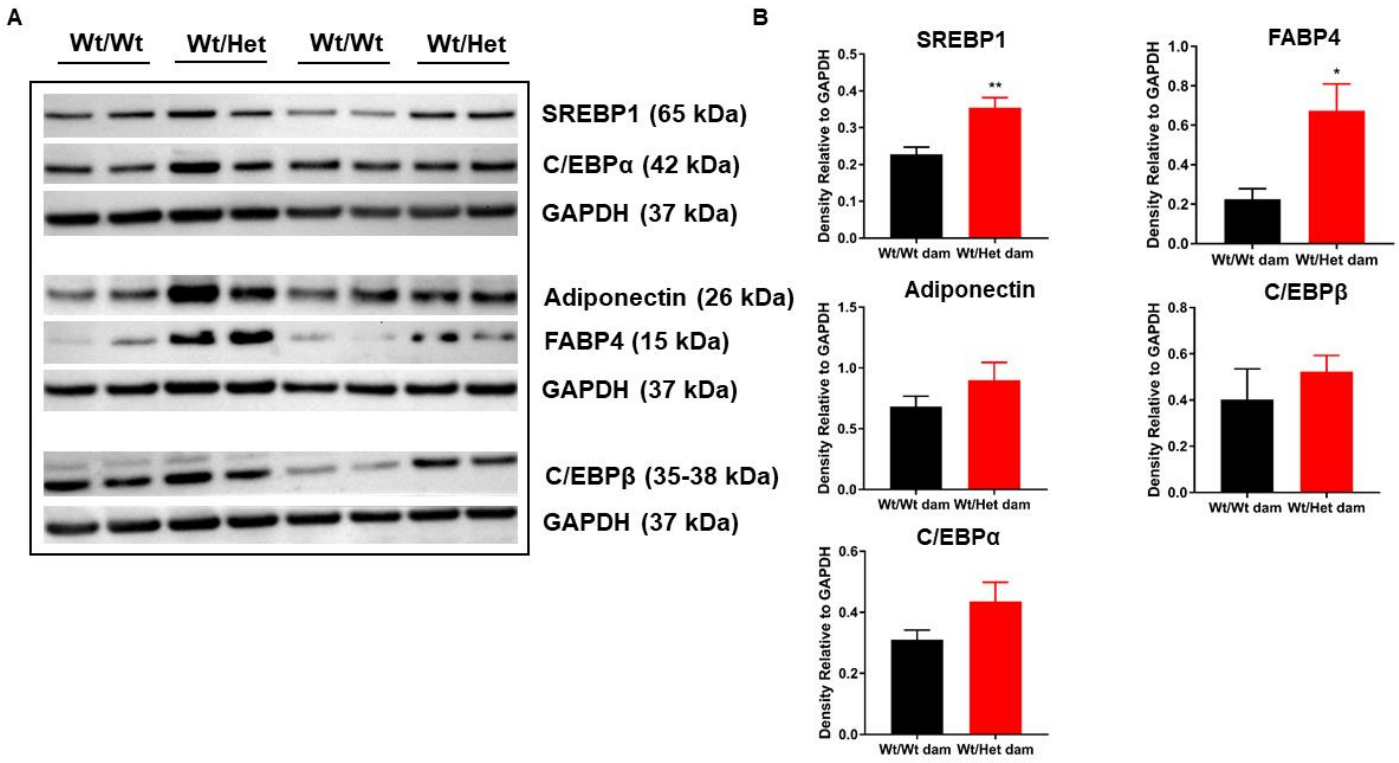

Figure 8. Higher protein expression of adipogenic mediators in differentiated progenitor cells isolated from neonates exposed to a metabolically compromised in utero environment. Western Blot was used to examine the protein expression of adipogenic mediators in progenitors isolated from the SVF of male neonatal iSAT on Day 2 of differentiation (A). The protein expression was quantified relative to GAPDH (B). n = 4 pregnancies/group. * $p < 0.05$ Wt neonates born to Wt dams (Wt/Wt dam) vs. Wt neonates born to Het_{db} dams (Wt/Het dam). Differences were determined by Student's t-test.

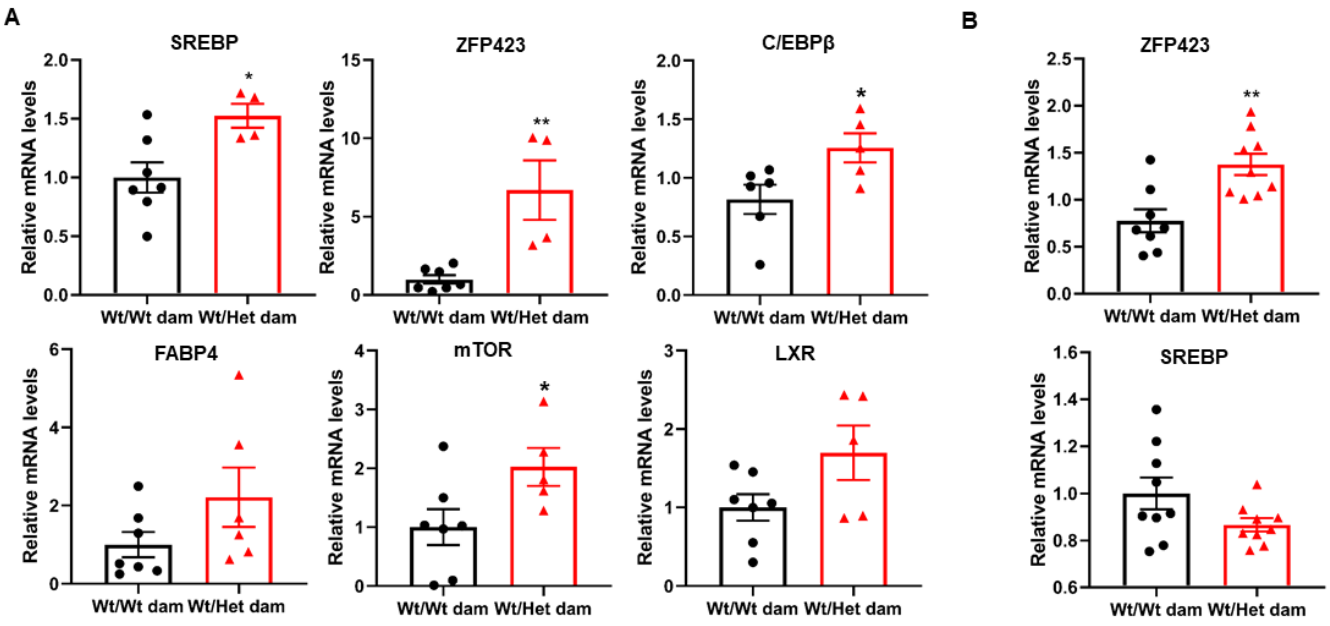

Figure 9. Higher mRNA expression of adipogenic markers in progenitor cells isolated from neonates exposed to a metabolically adverse in utero environment. mRNA levels of adipogenic genes were quantified using qPCR in Day 2 (A) and undifferentiated (B) progenitors isolated from the SVF of male neonatal iSAT. Gene expression was calculated relative to the reference gene, β-actin. n = 4-9 pregnancies/group. * $p < 0.05$ Wt neonates born to Wt dams (Wt/Wt dam) vs. Wt neonates born to Het_{db} dams (Wt/Het dam). Data was analyzed by Student's t-test.

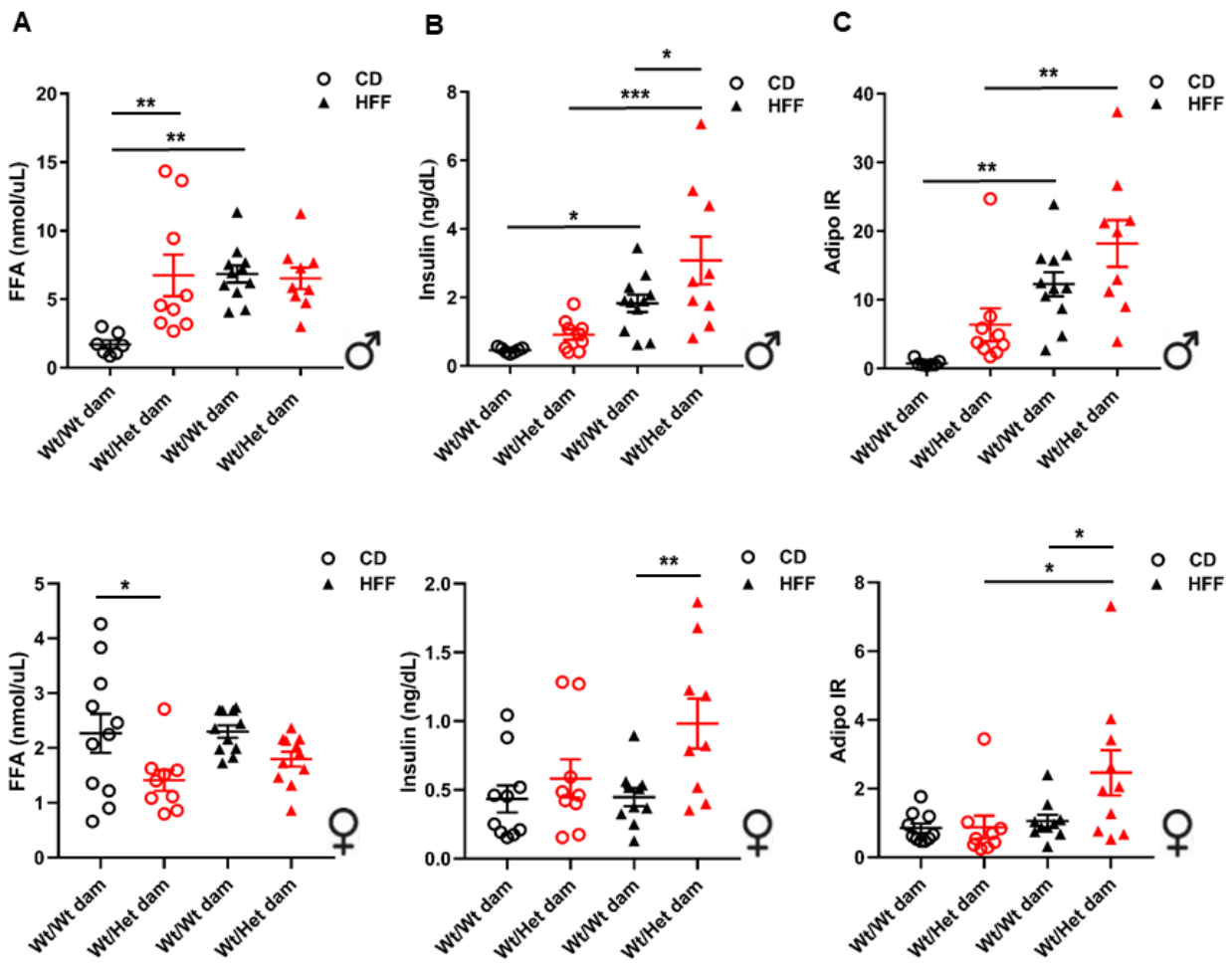

Figure 10. Perturbed whole-body lipid handling and lipid spillover in adult offspring born to dams with maternal metabolic dysfunction. Plasma free fatty acid (FFA) (A) and insulin (B) levels were measured in the fed state using a Colorimetric assay in adults placed on either a control diet (CD) or a high fat/fructose (HFF) diet. Adipose tissue insulin resistance (Adipo-IR) (C) was determined by calculating FFAs x insulin. n = 9-11 pregnancies/group. * $p < 0.05$ Wt offspring born to Wt dams (Wt/Wt dam) vs. Wt offspring born to Het_{db} dams (Wt/Het dam). Two-way ANOVA followed by Sidak's Multiple Comparisons test were performed.

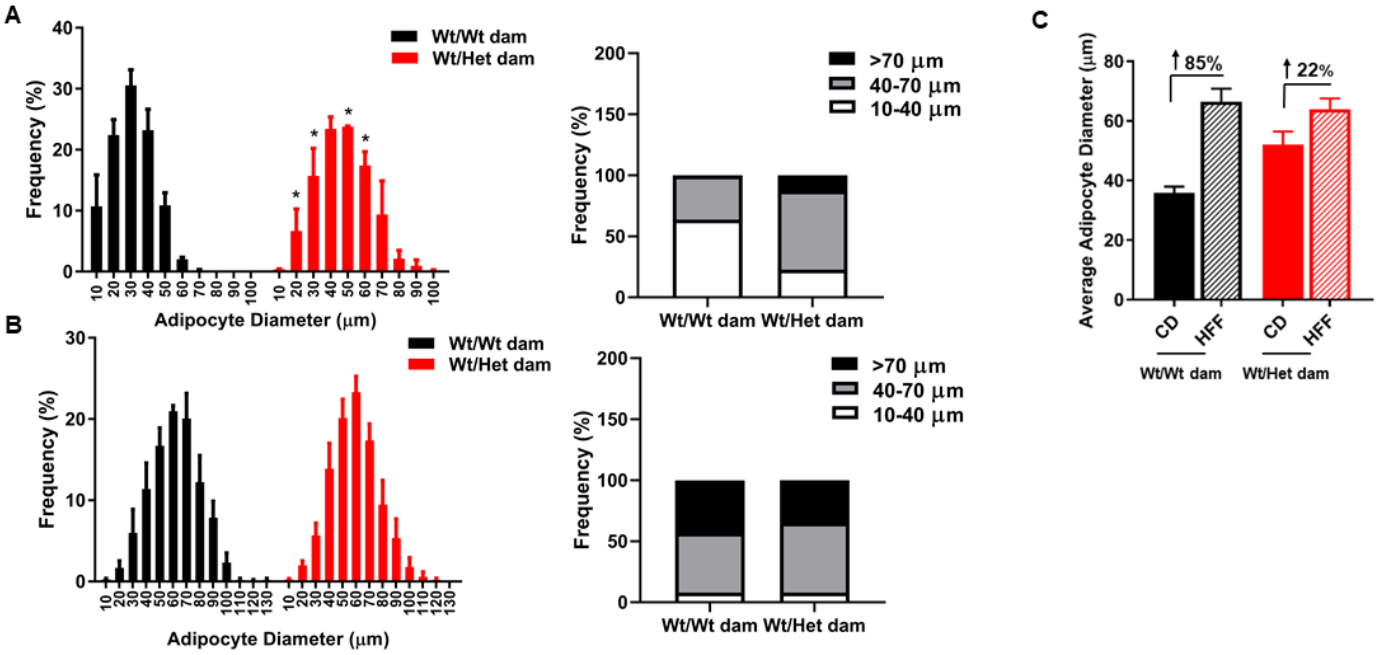

Figure 11. Greater adipocyte hypertrophy in iSAT of adults exposed to a metabolically compromised pregnancy. Adiposoft (ImageJ) software was utilized to examine the cell size distribution in H&E-stained sections of iSAT isolated from male and female adults placed on a control diet (CD) (A) or a high fat/fructose (HFF) diet (B). Average iSAT cell size was determined in offspring fed a CD vs. HFF diet (C). Male and female offspring from 3 pregnancies were included in each group. * $p < 0.05$ Wt offspring born to Wt dams (Wt/Wt dam) vs. Wt offspring born to Het_{db} dams (Wt/Het dam). Two-way ANOVA followed by Sidak's Multiple Comparisons test. [Data was generated by Dr. Jennifer Thompson]

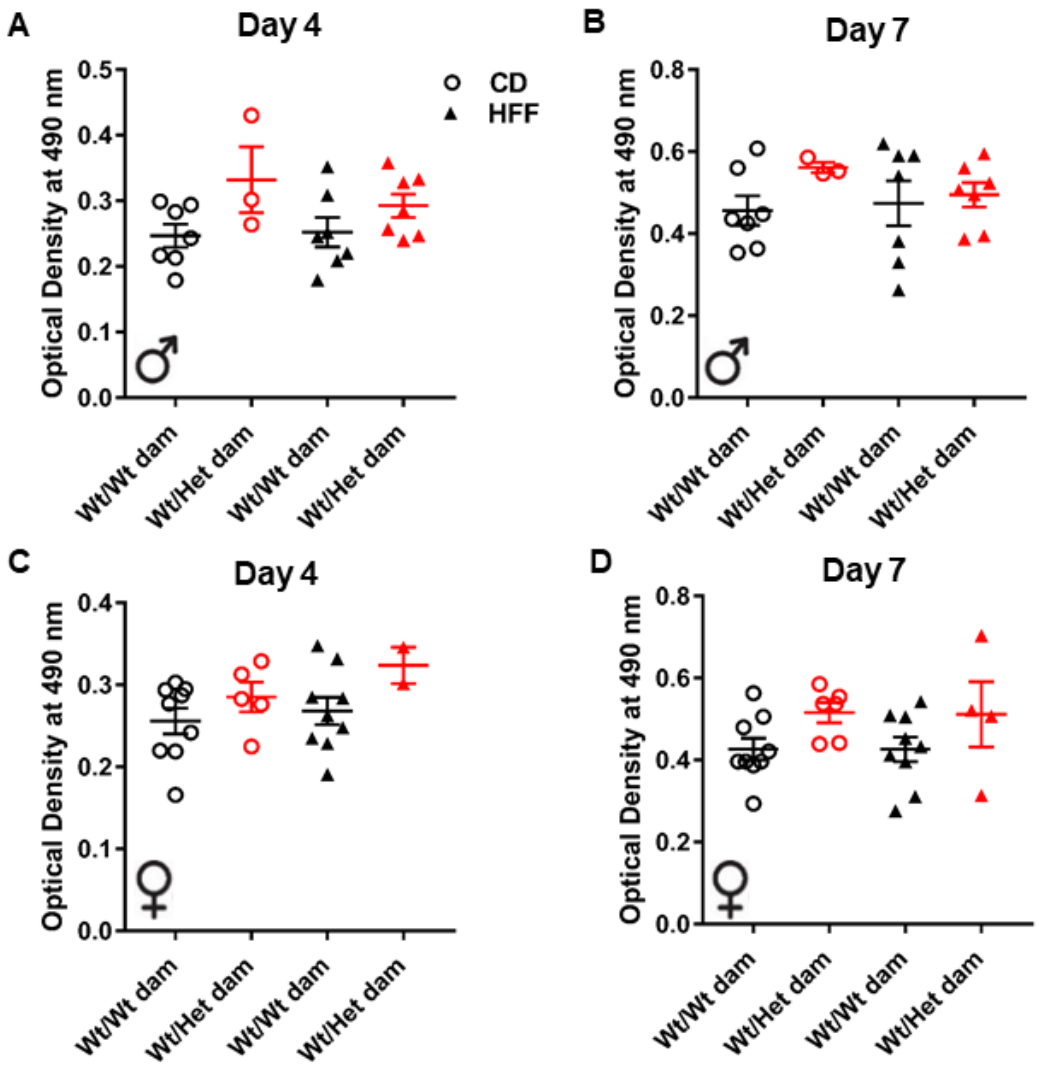

Figure 12. Differentiation capacity is not impeded in adults exposed to maternal metabolic dysfunction. Oil Red O staining was performed on progenitors isolated from the SVF of iSAT in adults fed a control diet (CD) or a high fat/fructose (HFF) diet. Lipid droplet formation was quantified by optical density on Day 4 (A) (C) and Day 7 (B) (D) of differentiation. n = 2-8 pregnancies/group. * $p < 0.05$ Wt offspring born to Wt dams (Wt/Wt dam) vs. Wt offspring born to Het_{db} dams (Wt/Het dam). Two-way ANOVA followed by Sidak's Multiple Comparisons test.

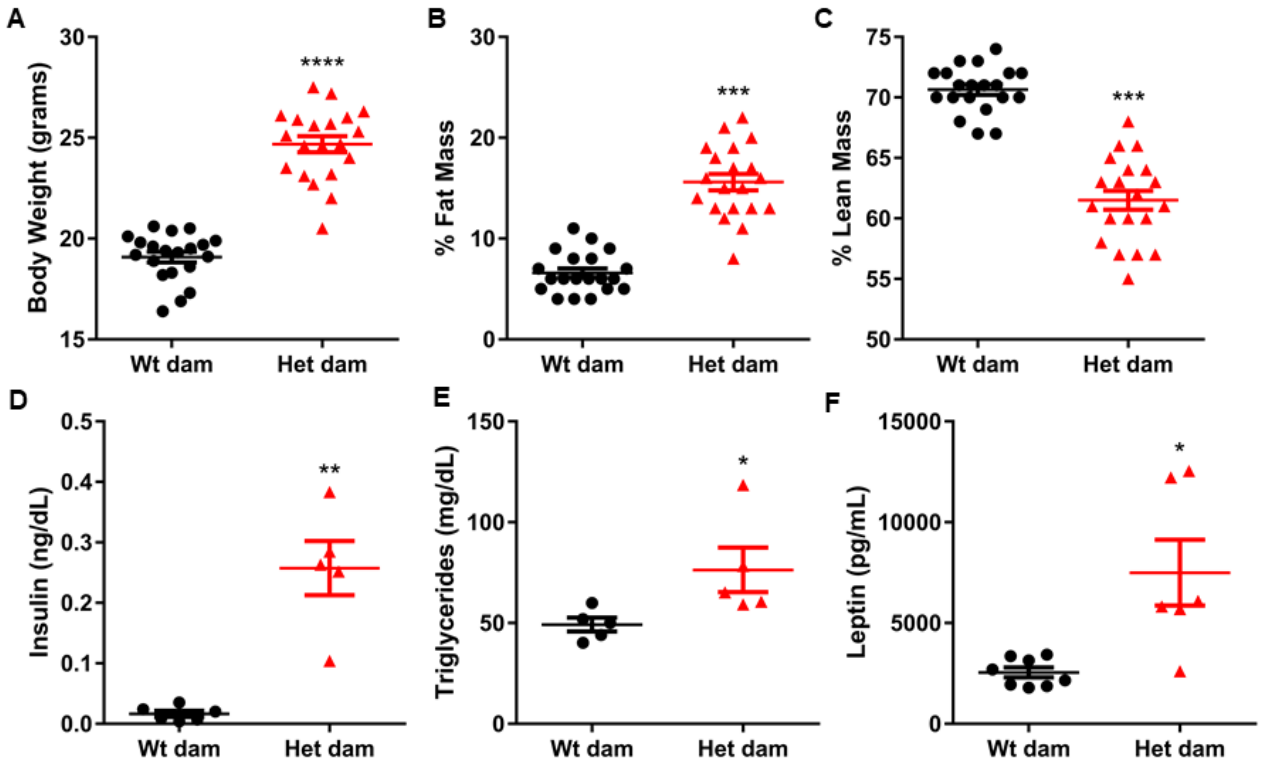

Supplementary Figure 1. Metabolic dysfunction is present in female mice heterozygous for leptin receptor deficiency. Prior to mating, body weight (A) was measured and a TD-NMR whole-body composition analyzer was used to calculate percent fat mass (B) and percent lean mass (C) in 14-week old virgin female mice (n = 20 pregnancies/group). Fasting levels of insulin (D), triglycerides (E) and leptin (F) were assessed in the plasma on Gd17 of pregnancy (n = 5-8 pregnancies/group) using Colorimetric assays. * $p < 0.05$ Wt (wild type) vs. Het (leptin receptor deficiency). Differences were determined by Student's t-test. [Data was generated by Dr. Jennifer Thompson]

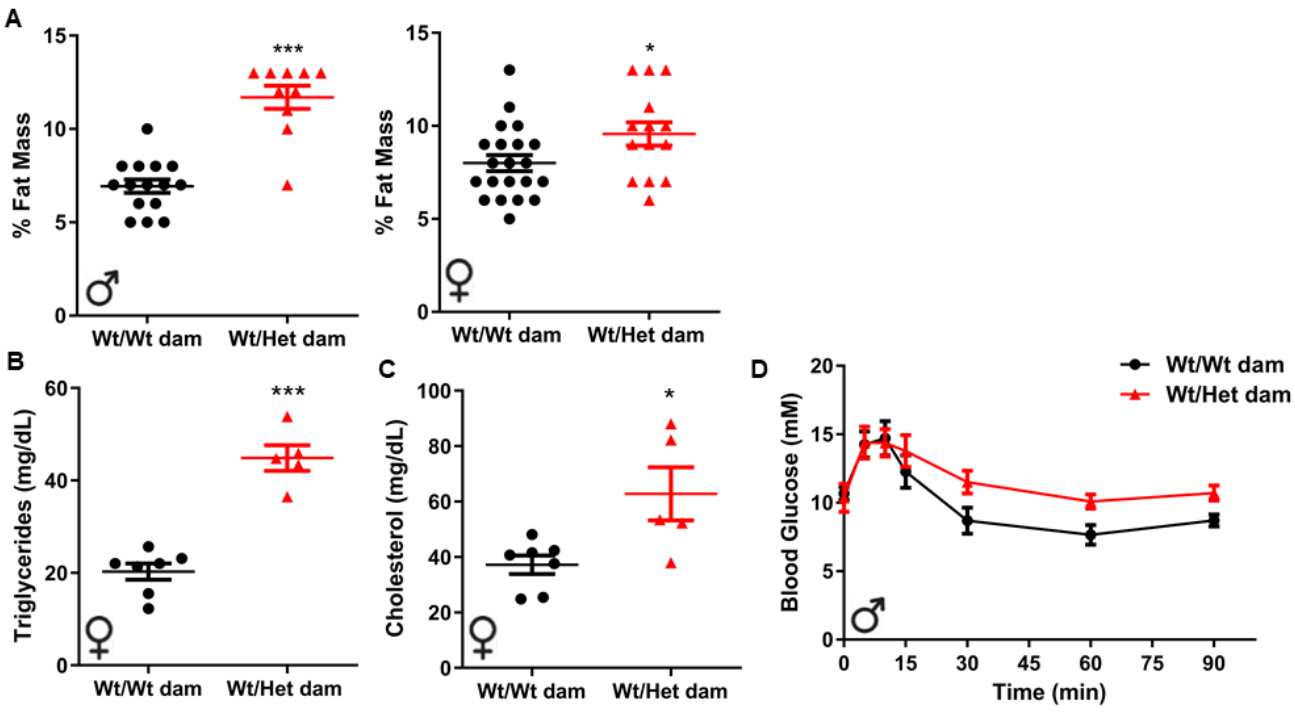

Supplementary Figure 2. Exposure to metabolically compromised dams predisposes offspring to develop adverse outcomes associated with CVD. In adult offspring, percent fat mass (A) was assessed using a TD-NMR whole-body composition analyzer (data shown includes the remaining offspring from 8-12 pregnancies/group that had body composition analyzed as neonates). Colorimetric assays were utilized to evaluate triglycerides (B) and cholesterol (C) in the plasma of adults (n = 5-7 pregnancies/group). Following a 6 hour fast, insulin sensitivity (D) was examined by measuring blood glucose levels in the tail in response to an IP injection of 0.5 IU/kg insulin (n = 3-5 pregnancies/group). * $p < 0.05$ Wt offspring born to Wt dams (Wt/Wt dam) vs. Wt offspring born to Het_{db} dams (Wt/Het dam). Student's t-test for A, B and C; Two-way ANOVA followed by Sidak's Multiple Comparisons test for D. [A, B and C were generated by Dr. Jennifer Thompson; D was generated by Dr. Nada Sallam]

Gene		Sequence	Accession
SREBP1	Forward	AACTTTTCCTTAACGTGGGC	NM_011480.4
	Reverse	CATGTCTTCGATGTCGTTCA	
ZFP423	Forward	AACAAAGTTTCCGAGAGGC	NM_033327.2
	Reverse	CCCTCTTCAACTTTCACCGA	
C/EBPβ	Forward	CAACACACGTGTAACTGTCA	NM_001287738.1
	Reverse	CGAAACGGAAAAGGTTCTCA	
FABP4	Forward	GACAAGCTGGTGGTGGAATGTG	NM_024406.3
	Reverse	CCATCCAGGCCTCTTCCTTTG	
mTOR	Forward	TATCCGCTACTGTGTCTTGG	NM_020009.2
	Reverse	TGCTCCTTGATTCTCCCAAT	
LXR	Forward	AGAGAGATGGAACTAGACCG	AJ132599.1
	Reverse	TAGCTTCCCCACCAGACTAA	
B-actin	Forward	GATCAAGATCATTGCTCCTCCT	XM_030254057.1
	Reverse	GTAACAGTCCGCCTAGAAGC	

Supplementary Table 1. Primer Sequences. The primer sequences are listed for each gene analyzed with q-PCR.

Chapter 4: Discussion, Conclusion, Limitations and Future Directions

Discussion

The overarching hypothesis for this study is that perturbed adipose tissue development leading to later-life impairment in SAT expandability underlies the development of CVD risk factors in offspring born to metabolically compromised pregnancies. My research project aimed to 1) determine the effect of maternal metabolic dysfunction on developmental adipogenesis and 2) determine if adipose tissue dysfunction underlies the development of CVD risk in offspring born to dams with metabolic dysfunction.

The concept of fetal programming proposes that the in utero environment plays a pivotal role in lifelong health and risk for disease (Marciniak et al., 2017). Gestational exposure to maternal metabolic dysfunction, such as obesity (Bayol et al., 2008) and diabetes (Bunt et al., 2005), is associated with the development of obesity and other CVD risk factors in the offspring. In this study, a mouse model was utilized to reproduce the characteristics of maternal metabolic disease to examine its impact on adipose tissue development and later-life lipid metabolism in the offspring. The presence of maternal metabolic dysfunction was confirmed by comparing wild type (Wt) control females to females heterozygous for leptin receptor deficiency (Het_{db}). Pre-pregnancy results revealed a higher body weight, an increase in whole-body fat mass and a decrease in lean body mass in Het_{db} vs. Wt females, highlighting the existence of high pre-pregnancy adiposity in Het_{db} females. High pre-pregnancy BMI in human women has been shown to impact developmental outcomes in the offspring (Heslehurst et al., 2019) and is a risk factor for GDM (Hashim et al., 2019). Insulin, a hormone released by the pancreatic β-cells, is a key regulator of glucose (Wilcox, 2005). In comparison to Wt females, Het_{db} females had higher levels of insulin in the plasma on gestational day 17 (Gd17). Hyperinsulinemia in the Het_{db}

females is suggestive of insulin resistance, which occurs when the body is unable to respond to the metabolic effects of insulin (Shanik et al., 2008). Triglycerides can be obtained by processing dietary fats in the small intestine or they can be synthesized from glycerol and free fatty acids (FFAs) in the liver (Toth, 2016). Lipoproteins, such as chylomicrons and very-low-density lipoprotein (VLDL), facilitate the transport of triglycerides in the plasma (Toth, 2016). Lipoprotein lipase releases FFAs from the triglyceride-rich lipoproteins (Toth, 2016). The FFAs can then be oxidized in the muscle or stored in the adipose tissue (Toth, 2016). Denke et al. reported that an increase in BMI was associated with elevated triglycerides in Caucasian American women (Denke, Sempos, & Grundy, 1994). In addition, Ryckman et al. revealed that there was a rise in triglycerides in women with vs. without GDM in all three trimesters of pregnancy (K. Ryckman, Spracklen, Smith, Robinson, & Saftlas, 2015). Our results showed that Het_{db} females exhibited higher levels of plasma triglycerides on Gd17 in comparison to Wt females. Maternal triglycerides are hydrolyzed into free fatty acids by placental enzymes and can thereby cross the placenta and enter fetal circulation (Hulme et al., 2019). A study conducted by Olmos et al. proposed that increased maternal triglycerides could lead to macrosomia in the infant (Olmos et al., 2014). High maternal triglycerides in overweight and obese mothers with GDM were associated with LGA offspring (Olmos et al., 2014). Leptin, a hormone secreted by the adipose tissue, is essential for sustaining the balance of energy stores (Klok, Jakobsdottir, & Drent, 2007). In response to a surplus of energy, leptin promotes appetite suppression and heightens metabolic rate (Schwartz et al., 2003). Studies have shown a rise in leptin in mothers with obesity and GDM (Carlhäll et al., 2016) (Kautzky-Willer et al., 2001). Consistent with this finding, our results revealed elevated levels of plasma leptin in Het_{db} vs. Wt females on Gd17. Al Maskari et al. demonstrated that high leptin levels were linked to increases in body weight, body

fat percentage and BMI in obese subjects (Al Maskari & Alnaqdy, 2006). Leptin resistance has been proposed as an explanation for the hindered capacity of leptin to maintain energy homeostasis in individuals suffering from obesity (Myers et al., 2012). Liu et al. reported that GDM mothers exhibited elevated levels of leptin, which were associated with a rise in insulin resistance (Liu, Fang, Yang, & Liu, 2012). Leptin measurements in cord blood have been shown to predict fetal growth (Perng et al., 2017). Therefore, the Het_{db} model creates a consistent and reproducible level of maternal metabolic dysfunction including high pre-pregnancy adiposity, gestational hyperinsulinemia, hypertriglyceridemia and hyperleptinemia. All of these metabolic derangements are common in human pregnancies complicated by maternal obesity or GDM and thus, the Het_{db} model reproduces the adverse intrauterine environment responsible for programming of CVD risk factors in human offspring.

In order to explore the long-term consequences of maternal metabolic dysfunction, risk factors for CVD were assessed in adult offspring fed a chow diet. Metabolic syndrome, a salient instigator of CVD, is comprised of several morbidities, including obesity, dyslipidemia, hypertension and insulin resistance (Huang, 2009). NMR spectroscopy results demonstrated that whole-body fat mass was higher in Wt males and females from the Het_{db} vs. Wt pregnancy, which suggests that offspring born to metabolically compromised dams have a greater susceptibility to become obese. Dyslipidemia is identified when triglycerides and high-density lipoprotein (HDL) cholesterol are increased and decreased, respectively (Alberti et al., 2009). In comparison to adults born to the Wt dam, plasma triglycerides and total cholesterol were elevated in older female adults born to the Het_{db} dam. Older male adults were not readily available at the time, therefore, triglycerides and total cholesterol were not assessed in the plasma of males. This data illustrates the presence of hypertriglyceridemia and hypercholesterolemia,

indicative of dyslipidemia, in females exposed to maternal metabolic dysfunction. Insulin resistance occurs when the cells lose their capacity to respond to the action of insulin (Shanik et al., 2008). During an insulin tolerance test, male offspring from the Het_{db} pregnancy exhibited increased levels of glucose after receiving an intraperitoneal (IP) injection of insulin, suggesting impaired insulin sensitivity. Unlike the males, female offspring did not experience differences in insulin sensitivity. Our results reveal that adult offspring born to metabolically compromised pregnancies possess a phenotype reflective of metabolic syndrome, including obesity, dyslipidemia and insulin resistance. Metabolic syndrome has been identified as a precipitator of CVD (Huang, 2009). Therefore, our data suggest that the maternal metabolic dysfunction present in the Het_{db} model programs the development of CVD risk factors in adult offspring, similar to human offspring born to women with metabolic disease during pregnancy.

Aim 1 of my research project was to determine the effect of maternal metabolic dysfunction on developmental adipogenesis. Maternal obesity and GDM have been linked to complications in fetal development (Kc et al., 2015). A common adverse outcome that occurs in infants is macrosomia, a condition in which the birth weight exceeds 4000 grams (Kc et al., 2015). Catalano et al. reported that the presence of obesity and GDM during pregnancy had both an independent and synergistic effect on birth weight and newborn percent body fat (both > 90^{th} percentile) (Catalano et al., 2012). Childhood obesity has been recognized as a stimulus for the emergence of CVD risk factors in adults, which include glucose intolerance, hypertension, dyslipidemia and inflammation (Nadeau et al., 2011). Therefore, the risk of developing CVD in the future could stem from a greater formation of fat in early life (Nadeau et al., 2011). In a lineage tracing study, Wang et al. demonstrated that mice accumulate subcutaneous fat between gestational days 14 and 18, while fat in the visceral depot develops after birth (Wang et al.,

2013). Since the formation of the subcutaneous depot is initiated in utero, a healthy pregnancy may be critical in establishing SAT depots that will maintain lipid homeostasis throughout the lifespan (Wang et al., 2013). Our results revealed that 3-week old Wt male and female neonates born to the Het_{db} vs. Wt pregnancy had a higher whole-body fat mass, which confirms that Het_{db} pregnancy reproduces the excessive accumulation of fetal fat mass characteristic of pregnancies complicated by maternal obesity or GDM (Kc et al., 2015). In addition, neonates exposed to the Het_{db} dam had higher levels of total free fatty acids (FFAs), which were positively correlated with whole-body fat mass. Resistin is mainly released by mature adipocytes in mice and by immune cells in humans (Sánchez-Solana, Laborda, & Baladrón, 2012). Nieva-Vazquez et al. reported that elevated resistin levels were linked to an increase in body fat percentage and a decrease in insulin sensitivity in obese Hispanic individuals (Nieva-Vazquez, Pérez-Fuentes, Torres-Rasgado, López-López, & Romero, 2014). A similar relationship between adiposity and resistin was discovered in our model, in which female neonates from the Het_{db} vs. Wt pregnancy exhibited higher levels of resistin. Regardless of having a higher whole-body fat mass, males born to the Het_{db} dam did not experience differences in resistin. Our results provide evidence for heightened fat accumulation in neonates born to dams with metabolic dysfunction and indicate that sex-dependent effects may be playing a role in resistin secretion.

Fat accumulation occurs through the process of adipogenesis, which can be divided into two phases- determination and terminal differentiation (Urrutia et al., 2018). In the determination stage, mesenchymal stem cells become committed to the adipocyte lineage through the generation of preadipocytes (Urrutia et al., 2018). During terminal differentiation, the preadipocytes differentiate into mature adipocytes that contain lipid droplets (Urrutia et al., 2018). Based on existing in vitro studies, our speculation is that insulin drives the accumulation

of fetal fat mass through stimulating adipogenesis (Otto & Lane, 2005) (Ghaben & Scherer, 2019). The Pedersen hypothesis proposes that insulin production in the fetus is elevated in response to maternal hyperglycemia (Kc et al., 2015). Consequently, fetal hyperinsulinemia increases the accretion of fat and protein, leading to the development of macrosomia in the infant (Kc et al., 2015). The Pedersen hypothesis is supported by a 2009 study, in which the researchers determined that increased levels of maternal glucose and cord serum C-peptide, a measure of fetal insulin, were linked to greater adiposity in the neonates (HAPO Study Cooperative Research Group, 2009). In addition to insulin, maternal lipids have been suggested as a stimulator of macrosomia (Di Cianni et al., 2005). Di Cianni et al. reported that higher levels of triglycerides in mothers with normal glucose tolerance were predictive of increased neonatal birth weights (Di Cianni et al., 2005). In order to assess the rate of adipogenesis, adipocyte diameter was measured in the iSAT of neonates. There was a shift in the cell size distribution from smaller adipocytes in neonates born to the Wt dam to larger adipocytes in neonates born to the Het_{db} dam, which suggests that adipogenesis occurs prematurely in offspring born to metabolically compromised pregnancies. It is possible that the shift in cell size in favour of larger adipocytes may be reflective of higher lipid droplet accumulation rather than an increase in adipogenesis. Therefore, an in vitro differentiation assay was performed to examine the adipogenic potential of progenitor cells. Stem cells isolated from the SVF of neonatal iSAT were plated, cultured and induced to differentiate after contact inhibition was established, a critical period in which the stem cells develop adipogenic potential (Zhang et al., 2009). Since male and female neonates had a similar phenotype in terms of body composition, we decided to proceed with the in vitro differentiation assay using only male neonates. In male neonates from the Het_{db} pregnancy, stem cells isolated from the iSAT exhibited higher lipid droplet accumulation on Day

2 and Day 4 of differentiation, as measured by Oil Red O staining. There was no difference in lipid droplet accumulation on Day 7 of differentiation. Western blot experiments revealed that Het_{db} pregnancy was associated with an increased expression of adipogenic mediators, fatty acid-binding protein 4 (FABP4) and sterol regulatory element-binding protein 1 (SREBP1), in Day 2 stem cells isolated from the iSAT of males. FABP4, a protein highly expressed in the adipose tissue, is an important modulator of lipid metabolism and inflammation (Hotamisligil & Bernlohr, 2015). It has been identified as a marker of adipocyte differentiation, in which the expression of FABP4 is regulated by PPARγ (Hotamisligil & Bernlohr, 2015). Similar to FABP4, SREBP1c expression is heightened in the adipose tissue (Payne et al., 2009). SREBP1c plays an active role in adipogenesis as an inducer of PPARγ (Payne et al., 2009). In addition, SREBP1c is a master regulator of lipogenic enzymes involved in lipogenesis and the formation of lipid droplets (Steffensen & Gustafsson, 2004). There was no difference in the protein expression of adiponectin, C/EBPα and C/EBPβ in Day 2 stem cells isolated from the neonatal iSAT. qPCR results demonstrated an increased mRNA expression of Zfp423 in undifferentiated stem cells, and an increased mRNA expression of Zfp423, SREBP1, C/EBPβ and mTOR in Day 2 stem cells isolated from the neonatal iSAT of males born to the Het_{db} dam. No differences were observed between the groups when examining mRNA levels of SREBP1 in undifferentiated stem cells, as well as mRNA levels of FABP4 and LXR in Day 2 stem cells. The data obtained from Oil Red O staining, Western blot and qPCR suggests that there is a higher adipogenic potential in progenitor cells isolated from neonates exposed to a metabolically compromised in utero environment. Our speculation is that either the cells have an increased intrinsic ability to differentiate or that there are a greater number of preadipocytes in the stem cell culture already primed for differentiation. In reference to the first aim of my study, the results from several

experiments provide evidence for accelerated developmental adipogenesis in neonates exposed to metabolic dysfunction.

Aim 2 of my research project was to determine if adipose tissue dysfunction underlies the development of CVD risk in offspring born to dams with metabolic dysfunction. The SAT functions as a metabolic sink to hinder the spillover of lipids into the VAT and non-adipose organs, including the liver, heart and skeletal muscle (Bjørndal et al., 2011) (Longo et al., 2019). A growing body of evidence suggests that an inability for the SAT to expand is involved in the pathogenesis of CVD risk factors (Bays, 2014). The adipose tissue expandability hypothesis states that the adipose tissue has a defined capacity to expand (Virtue & Vidal-Puig, 2010). Once the limit of expansion is reached, the adipose tissue becomes ineffective in handling lipid overload, leading to adipose tissue dysfunction (ATD) (Goossens & Blaak, 2015). ATD is recognized by various characteristics, including abnormal adipokine secretion, hypoxia, fibrosis, inflammation and insulin resistance (Goossens & Blaak, 2015) (Sun et al., 2013). The development of insulin resistance was investigated to confirm the presence of dysfunctional adipocytes. In healthy adipose tissue, insulin is an inhibitor of lipolysis (Virtue & Vidal-Puig, 2010), a process that occurs when triglycerides are converted into free fatty acids (FFAs) for utilization by other tissues (Coelho et al., 2013). Insulin resistant adipocytes lose this insulin-mediated inhibition, resulting in increased lipolysis (Virtue & Vidal-Puig, 2010). There is a subsequent accumulation of lipids in ectopic tissues, generating a state of lipotoxicity (Virtue & Vidal-Puig, 2010). Therefore, an increase in both insulin and FFAs is indicative of insulin resistance (Virtue & Vidal-Puig, 2010). A rise in the level of FFAs has been linked to the development of CVD risk factors, including myocardial impairments, high blood pressure and atherosclerosis (Pilz & März, 2008). In offspring fed a control diet (CD), FFAs were elevated in

males born to Het_{db} pregnancies. The high fat/fructose (HFF) diet was associated with a higher level of FFAs in the plasma of Wt male adults born to the normal pregnancy, but led to no further increases in males born to Het_{db} pregnancies. In response to the HFF diet, insulin and adipose tissue insulin resistance (Adipo-IR), a measure of the ability of adipose tissue to suppress lipolysis in response to insulin, increased in male adults from both pregnancies. These results indicate that there is an attenuated insulin-induced inhibition of lipolysis in male adults exposed to an obesogenic diet. Even though the difference in Adipo-IR between male offspring did not reach significance, males born to the Het_{db} vs. Wt pregnancy had elevated levels of insulin when fed a HFF diet. In contrast, exposure to the Het_{db} dam was associated with a drop in FFAs in CD-fed female adults. In the Het_{db} dam, female adults exhibited an increase in Adipo-IR following the consumption of a HFF diet. Furthermore, HFF diet-fed female offspring from the Het_{db} vs. Wt pregnancy had higher insulin levels and Adipo-IR. These findings suggest that exposure to the Het_{db} pregnancy exacerbates the HFF-diet induced increase in ATD in female offspring. This data sets forth the notion that whole-body lipid handling and the lipolytic response to insulin is compromised in adults born to metabolically adverse pregnancies.

SAT expansion is fundamental for coping with a surplus of calories (Longo et al., 2019). The SAT has the capacity to expand by utilizing the mechanisms of hyperplasia and hypertrophy (Longo et al., 2019). Hyperplasia and hypertrophy are defined as increases in adipocyte number and size, respectively (Longo et al., 2019). An impaired ability to form new adipocytes from an existing population of preadipocytes leads to the hypertrophic-induced dysfunction of mature adipocytes, followed by lipid spillover into the bloodstream (Longo et al., 2019). In order to investigate the recruitment of preadipocytes for differentiation, adipocyte diameter was measured in the iSAT of adults fed a CD and HFF diet. In Wt adults fed a CD, Het_{db} pregnancy was

associated with a lower number of smaller-sized adipocytes and a rise in larger-sized adipocytes. This finding suggests that adults exposed to a metabolically compromised pregnancy have greater adipocyte hypertrophy in the absence of HFF feeding. Exposure to the HFF diet led to an even greater reduction in smaller-sized adipocytes and a higher frequency of larger-sized adipocytes in offspring born to both dams. The HFF diet abolished adipocyte diameter differences between the Wt and Het_{db} pregnancies. Adipocytes in the iSAT of adult offspring were able to enlarge by 85% and 22% in Wt and Het_{db} dams, respectively, when fed a HFF diet. This result suggests that the Het_{db} adipocytes were hypertrophic prior to HFF diet exposure, resulting in a compromised ability to expand in response to caloric challenge. The buffering capacity of the SAT can become impaired due to 1) a blunted capacity for the preadipocytes to differentiate (Isakson et al., 2009) or 2) a depletion in the preadipocyte supply (Tchoukalova et al., 2007). The preadipocyte population that gives rise to new adipocytes in adulthood originates from a pool of cells that become committed during gestation (Jiang et al., 2014) (W. Tang et al., 2008). Isakson et al. determined that an increase in both BMI and adipocyte cell size was associated with a reduced number of preadipocytes that could differentiate into mature adipocytes (Isakson et al., 2009). In addition, a rise in BMI was linked to a higher number of CD133-positive cells, which are a population of SVF progenitor cells with the capacity to differentiate into adipose, muscle and bone cells (Isakson et al., 2009). These findings suggest that obese individuals do not lack an adequate supply of multipotent progenitors, rather, preadipocyte commitment and/or the differentiation capacity of the preadipocytes is compromised (Isakson et al., 2009). Chatterjee et al. reported that a chronic HFD hindered the differentiation capacity of murine cells, which resulted in the subsequent formation of dysfunctional adipocytes unfit to store lipids (Chatterjee et al., 2014). In contrast to the

Chatterjee study, our results revealed that HFF feeding did not effect the adipogenic potential of stem cells present in the SVF of iSAT. We also did not observe any differences in the intrinsic differentiation capacity in isolated progenitor cells from offspring born to Het_{db} dams. Therefore, our results suggest that the differentiation capacity is not impeded in adults exposed to maternal metabolic dysfunction. Since our experiment examined differentiation in isolated stem cells that were enriched and induced, this result does not preclude the possibility that preadipocyte numbers were reduced in iSAT depots or that in vivo differentiation capacity is impaired in the native environment. Tchoukalova et al. determined that obese individuals had a lower frequency of committed preadipocytes in the SAT (Tchoukalova et al., 2007). Future studies will determine if a depletion in the preadipocyte pool is the mechanism responsible for impaired SAT function in adult offspring.

The sex of the offspring needs to be considered in the assessment of observed outcomes. Although similarities between males and females exist, there are several sex differences that are worth addressing. Unlike the males, female neonates born to the Het_{db} vs. Wt dam exhibited elevated levels of resistin. Similar to this finding, Norata et al. demonstrated that plasma resistin levels were upregulated in women with vs. without metabolic syndrome (Norata et al., 2007). Meanwhile, the presence of metabolic syndrome did not alter resistin levels in the men (Norata et al., 2007). In the adult offspring, sex differences were present when examining the diet and pregnancy effects. Overall, the males appear to experience greater metabolic impairments in response to the HFF diet, whereas the females are protected from the diet effects. This is evident in our results, which demonstrated that the HFF diet increased FFAs in male adults born to the Wt dam. In addition, insulin levels and Adipo-IR measurements were elevated in response to the HFF diet in male offspring from both the Wt and Het_{db} pregnancy. Unlike the males, the HFF

diet only increased the Adipo-IR in females born to the Het_{db} dam. Estrogen may be playing a critical role in protecting the females from diet-induced impairments (Stubbins, Najjar, Holcomb, Hong, & Núñez, 2012). Stubbins et al. reported the beneficial effects of estrogen in HFD-fed female mice, as demonstrated by a reduction in adipocyte size, lower oxidative stress and inflammation in the adipocytes, and the prevention of insulin resistance (Stubbins et al., 2012). In addition, the protective effects present in females could be due to a higher adipogenic response during high fat diet feeding (Greenhill, 2016) (Jeffery et al., 2016). With regards to the type of pregnancy, various metabolic changes were observed in the males and females. FFA levels were elevated in CD-fed male adults born to the Het_{db} vs. Wt pregnancy. In contrast, CD-fed females were protected from the pregnancy effect, as demonstrated by a lower level of FFAs in CD-fed female offspring exposed to the Het_{db} dam. However, exposure to the Het_{db} pregnancy was associated with increased insulin levels in both males and females on the HFF diet.

Conclusion

The data collected supports the following overarching hypothesis: impaired SAT expandability underlies the development of CVD risk factors in offspring born to metabolically compromised pregnancies. Aim 1 of my study was to determine the effect of maternal metabolic dysfunction on developmental adipogenesis. Our results provide evidence of accelerated developmental adipogenesis in neonates born to dams with metabolic dysfunction. Aim 2 of my study was to determine if adipose tissue dysfunction underlies the development of CVD risk in offspring born to dams with metabolic dysfunction. A metabolically adverse pregnancy is associated with the hallmarks of adipose tissue dysfunction, including lipid spillover and impaired insulin-stimulated inhibition of lipolysis. Our data suggests that the intrinsic differentiation capacity of adipocyte-derived stem cells was not the mechanism responsible for impaired SAT function. In conclusion,

intrauterine exposure to metabolic dysfunction leads to accelerated developmental adipogenesis and a later-life perturbation in lipid handling. Therefore, CVD risk may arise from SAT dysfunction programmed during the critical perinatal window of SAT development.

Limitations

It is critical to acknowledge that limitations exist in several areas of my research project. There is an inherent difference between animal and human studies, therefore, the observations in our mouse model might not be identical to the responses that are produced in humans. For example, insulin sensitivity differences have been reported when comparing adipose tissue depots in female mice and humans (Chusyd, Wang, Huffman, & Nagy, 2016). In human females, the SAT in the gluteofemoral region has a greater insulin sensitivity than VAT (Chusyd et al., 2016). Unlike humans, female mice experience a higher insulin sensitivity in the periovarian VAT compared to the inguinal SAT (Chusyd et al., 2016). Further, although iSAT development primarily occurs in late gestation in both human and mice (Wang et al., 2013), human infants are born with a greater amount of fat mass. Thus, a change in the intrauterine metabolic milieu may have a more severe impact on human offspring. Although the Het_{db} model captures the heterogeneity of maternal metabolic disease, it does not allow for the identification of specific effects that the different metabolic derangements have on adverse developmental outcomes. High maternal triglycerides (Di Cianni et al., 2005) and fetal hyperinsulinemia, in response to maternal hyperglycemia (Kc et al., 2015), have been recognized as risk factors in the development of macrosomia. Our model cannot determine if the excess fat accumulation in offspring is due to maternal glucose or lipid levels. Finally, cross-fostering was not performed, therefore lactation effects due to Het_{db} pregnancy are possible and may contribute to higher neonatal adiposity.

Regardless, our study shows that higher accumulation of fat mass during the critical perinatal window of iSAT development is associated with later-life perturbations in lipid metabolism.

Future Directions

The prevalence of maternal obesity and diabetes is associated with the early-onset of CVD risk factors in the offspring. Our data suggests that impaired SAT function, due to accelerated adipogenesis in utero, underlies the manifestation of adverse cardiovascular outcomes later on in life. The insulin signaling cascade is a promising area to explore as a potential mechanism responsible for the developmental programming of preadipocytes. In vitro studies have identified insulin as a potent inducer of adipogenesis in the adipose tissue (Otto & Lane, 2005). Fetal hyperinsulinemia has been recognized as the key link between maternal hyperglycemia and neonatal adiposity (HAPO Study Cooperative Research Group, 2009). Therefore, the role of insulin in adipogenesis could be further evaluated in the neonatal SAT and cells by examining the expression of markers present in the insulin signaling cascade, such as PI3K, mTOR, FOXO1 and LXR (Ghaben & Scherer, 2019) (Nakae et al., 2003) (Steffensen & Gustafsson, 2004). In order to quantify the population of committed preadipocytes in the stem cells, flow cytometry could be performed using cell surface markers specific to committed preadipocytes (Gao et al., 2017). Flow cytometry would allow us to determine if a depletion in preadipocyte supplies plays a role in SAT dysfunction. A comprehensive understanding of the mechanism involved in adipogenesis has the potential to provide insight into preventative strategies that could be implemented to minimize CVD risk in children born to metabolically compromised pregnancies.

References

Al Maskari, M. Y., & Alnaqdy, A. A. (2006). Correlation between Serum Leptin Levels, Body Mass Index and Obesity in Omanis. *Sultan Qaboos Univ Med J, 6*(2), 27-31. Retrieved from https://www.ncbi.nlm.nih.gov/pmc/articles/PMC3074914/pdf/squmj-06-27.pdf

Alberti, K. G. M. M., Eckel, R. H., Grundy, S. M., Zimmet, P. Z., Cleeman, J. I., Donato, K. A., . . . Smith, S. C. (2009). Harmonizing the Metabolic Syndrome. *Circulation, 120*(16), 1640-1645. doi:10.1161/CIRCULATIONAHA.109.192644

American Diabetes Association. (2019). 2. Classification and Diagnosis of Diabetes: Standards of Medical Care in Diabetes—2019. *Diabetes Care, 42*(Supplement 1), S13-S28. doi:10.2337/dc19-S002

Aref, A.-B. M., Ahmed, O. M., Ali, L. A., & Semmler, M. (2013). Maternal rat diabetes mellitus deleteriously affects insulin sensitivity and Beta-cell function in the offspring. *Journal of diabetes research, 2013*, 429154-429154. doi:10.1155/2013/429154

Baker, J. L., Olsen, L. W., & Sørensen, T. I. A. (2007). Childhood Body-Mass Index and the Risk of Coronary Heart Disease in Adulthood. *New England Journal of Medicine, 357*(23), 2329-2337. doi:10.1056/NEJMoa072515

Bayol, S. A., Simbi, B. H., Bertrand, J. A., & Stickland, N. C. (2008). Offspring from mothers fed a 'junk food' diet in pregnancy and lactation exhibit exacerbated adiposity that is more pronounced in females. *The Journal of Physiology, 586*(13), 3219-3230. doi:10.1113/jphysiol.2008.153817

Bays, H. (2014). Central obesity as a clinical marker of adiposopathy; increased visceral adiposity as a surrogate marker for global fat dysfunction. *Curr Opin Endocrinol Diabetes Obes, 21*(5), 345-351. doi:10.1097/med.0000000000000093

Bjørndal, B., Burri, L., Staalesen, V., Skorve, J., & Berge, R. K. (2011). Different Adipose Depots: Their Role in the Development of Metabolic Syndrome and Mitochondrial Response to Hypolipidemic Agents. *Journal of Obesity, 2011*, 490650. doi:10.1155/2011/490650

Boney, C. M., Verma, A., Tucker, R., & Vohr, B. R. (2005). Metabolic syndrome in childhood: association with birth weight, maternal obesity, and gestational diabetes mellitus. *Pediatrics, 115*(3), e290-296. doi:10.1542/peds.2004-1808

Buechler, C., Krautbauer, S., & Eisinger, K. (2015). Adipose tissue fibrosis. *World journal of diabetes, 6*(4), 548-553. doi:10.4239/wjd.v6.i4.548

Bunt, J. C., Tataranni, P. A., & Salbe, A. D. (2005). Intrauterine exposure to diabetes is a determinant of hemoglobin A(1)c and systolic blood pressure in pima Indian children. *The Journal of clinical endocrinology and metabolism, 90*(6), 3225-3229. doi:10.1210/jc.2005-0007

Butterwith, S. C., Wilkie, R. S., & Clinton, M. (1996). Treatment of pluripotential C3H 10T1/2 Fibroblasts with bone morphogenetic protein-4 induces adipocyte commitment. *Biochemical Society Transactions, 24*(2), 163S. doi:10.1042/bst024163s

Calkins, K., & Devaskar, S. U. (2011). Fetal origins of adult disease. *Current problems in pediatric and adolescent health care, 41*(6), 158-176. doi:10.1016/j.cppeds.2011.01.001

Carlhäll, S., Bladh, M., Brynhildsen, J., Claesson, I.-M., Josefsson, A., Sydsjö, G., . . . Blomberg, M. (2016). Maternal obesity (Class I-III), gestational weight gain and maternal leptin levels during and after pregnancy: a prospective cohort study. *BMC Obesity, 3*(1), 28. doi:10.1186/s40608-016-0108-2

Catalano, P. M., McIntyre, H. D., Cruickshank, J. K., McCance, D. R., Dyer, A. R., Metzger, B. E., . . . Oats, J. J. (2012). The hyperglycemia and adverse pregnancy outcome study: associations of GDM and obesity with pregnancy outcomes. *Diabetes Care, 35*(4), 780-786. doi:10.2337/dc11-1790

Chatterjee, T. K., Basford, J. E., Knoll, E., Tong, W. S., Blanco, V., Blomkalns, A. L., . . . Weintraub, N. L. (2014). HDAC9 knockout mice are protected from adipose tissue dysfunction and systemic metabolic disease during high-fat feeding. *Diabetes, 63*(1), 176-187. doi:10.2337/db13-1148

Chen, C., Xu, X., & Yan, Y. (2018). Estimated global overweight and obesity burden in pregnant women based on panel data model. *PLOS ONE, 13*(8), e0202183-e0202183. doi:10.1371/journal.pone.0202183

Cho, G. J., Kim, L. Y., Sung, Y. N., Kim, J. A., Hwang, S. Y., Hong, H.-R., . . . Kim, H.-J. (2015). Secular Trends of Gestational Diabetes Mellitus and Changes in Its Risk Factors. *PLOS ONE, 10*(8), e0136017. doi:10.1371/journal.pone.0136017

Choe, S. S., Huh, J. Y., Hwang, I. J., Kim, J. I., & Kim, J. B. (2016). Adipose Tissue Remodeling: Its Role in Energy Metabolism and Metabolic Disorders. *Frontiers in endocrinology, 7*, 30. doi:10.3389/fendo.2016.00030

Christodoulides, C., Lagathu, C., Sethi, J. K., & Vidal-Puig, A. (2009). Adipogenesis and WNT signalling. *Trends in endocrinology and metabolism: TEM, 20*(1), 16-24. doi:10.1016/j.tem.2008.09.002

Chu, S. Y., Callaghan, W. M., Kim, S. Y., Schmid, C. H., Lau, J., England, L. J., & Dietz, P. M. (2007). Maternal Obesity and Risk of Gestational Diabetes Mellitus. *Diabetes Care, 30*(8), 2070-2076. doi:10.2337/dc06-2559a

Chusyd, D. E., Wang, D., Huffman, D. M., & Nagy, T. R. (2016). Relationships between Rodent White Adipose Fat Pads and Human White Adipose Fat Depots. *Front Nutr, 3*, 10. doi:10.3389/fnut.2016.00010

Coelho, M., Oliveira, T., & Fernandes, R. (2013). Biochemistry of adipose tissue: an endocrine organ. *Archives of medical science : AMS, 9*(2), 191-200. doi:10.5114/aoms.2013.33181

Dabelea, D., Knowler, W. C., & Pettitt, D. J. (2000). Effect of diabetes in pregnancy on offspring: Follow-up research in the pima indians. *Journal of Maternal-Fetal Medicine, 9*(1), 83-88. doi:10.3109/14767050009020519

De Boo, H. A., & Harding, J. E. (2006). The developmental origins of adult disease (Barker) hypothesis. *Australian and New Zealand Journal of Obstetrics and Gynaecology, 46*(1), 4-14. doi:10.1111/j.1479-828X.2006.00506.x

de Luca, C., Kowalski, T. J., Zhang, Y., Elmquist, J. K., Lee, C., Kilimann, M. W., . . . Chua, S. C., Jr. (2005). Complete rescue of obesity, diabetes, and infertility in db/db mice by neuron-specific LEPR-B transgenes. *The Journal of clinical investigation, 115*(12), 3484-3493. doi:10.1172/JCI24059

Denke, M. A., Sempos, C. T., & Grundy, S. M. (1994). Excess Body Weight: An Under-recognized Contributor to Dyslipidemia in White American Women. *Archives of Internal Medicine, 154*(4), 401-410. doi:10.1001/archinte.1994.00420040061010

Di Cianni, G., Miccoli, R., Volpe, L., Lencioni, C., Ghio, A., Giovannitti, M. G., . . . Del Prato, S. (2005). Maternal triglyceride levels and newborn weight in pregnant women with normal glucose tolerance. *Diabetic Medicine, 22*(1), 21-25. doi:10.1111/j.1464-5491.2004.01336.x

Dimitriadis, G., Mitrou, P., Lambadiari, V., Maratou, E., & Raptis, S. A. (2011). Insulin effects in muscle and adipose tissue. *Diabetes Research and Clinical Practice, 93,* S52-S59. doi:https://doi.org/10.1016/S0168-8227(11)70014-6

Eriksson, J. G., Sandboge, S., Salonen, M., Kajantie, E., & Osmond, C. (2015). Maternal weight in pregnancy and offspring body composition in late adulthood: Findings from the Helsinki Birth Cohort Study (HBCS). *Annals of Medicine, 47*(2), 94-99. doi:10.3109/07853890.2015.1004360

Ferrara, A. (2007). Increasing Prevalence of Gestational Diabetes Mellitus. *A public health perspective, 30*(Supplement 2), S141-S146. doi:10.2337/dc07-s206

Flegal, K. M., Kruszon-Moran, D., Carroll, M. D., Fryar, C. D., & Ogden, C. L. (2016). Trends in Obesity Among Adults in the United States, 2005 to 2014. *JAMA, 315*(21), 2284-2291. doi:10.1001/jama.2016.6458

Fowden, A. L. (1992). The role of insulin in fetal growth. *Early Hum Dev, 29*(1-3), 177-181. doi:10.1016/0378-3782(92)90135-4

Fox, C. S., Massaro, J. M., Hoffmann, U., Pou, K. M., Maurovich-Horvat, P., Liu, C. Y., . . . O'Donnell, C. J. (2007). Abdominal visceral and subcutaneous adipose tissue compartments: association with metabolic risk factors in the Framingham Heart Study. *Circulation, 116*(1), 39-48. doi:10.1161/circulationaha.106.675355

Gaillard, R. (2015). Maternal obesity during pregnancy and cardiovascular development and disease in the offspring. *European journal of epidemiology, 30*(11), 1141-1152. doi:10.1007/s10654-015-0085-7

Gao, H., Volat, F., Sandhow, L., Galitzky, J., Nguyen, T., Esteve, D., . . . Bouloumié, A. (2017). CD36 Is a Marker of Human Adipocyte Progenitors with Pronounced Adipogenic and

Triglyceride Accumulation Potential. *Stem cells (Dayton, Ohio), 35*(7), 1799-1814. doi:10.1002/stem.2635

Ghaben, A. L., & Scherer, P. E. (2019). Adipogenesis and metabolic health. *Nature Reviews Molecular Cell Biology, 20*(4), 242-258. doi:10.1038/s41580-018-0093-z

Goossens, G. H., & Blaak, E. E. (2015). Adipose tissue dysfunction and impaired metabolic health in human obesity: a matter of oxygen? *Frontiers in endocrinology, 6*, 55. doi:10.3389/fendo.2015.00055

Greenhill, C. (2016). Sex differences in adipogenesis. *Nature Reviews Endocrinology, 12*(9), 497-497. doi:10.1038/nrendo.2016.109

Halberg, N., Khan, T., Trujillo, M. E., Wernstedt-Asterholm, I., Attie, A. D., Sherwani, S., . . . Scherer, P. E. (2009). Hypoxia-Inducible Factor 1α Induces Fibrosis and Insulin Resistance in White Adipose Tissue. *Molecular and Cellular Biology, 29*(16), 4467-4483. doi:10.1128/mcb.00192-09

Han, S., Sun, H. M., Hwang, K.-C., & Kim, S.-W. (2015). Adipose-Derived Stromal Vascular Fraction Cells: Update on Clinical Utility and Efficacy. *25*(2), 145-152. doi:10.1615/CritRevEukaryotGeneExpr.2015013057

HAPO Study Cooperative Research Group. (2009). Hyperglycemia and Adverse Pregnancy Outcome (HAPO) Study: associations with neonatal anthropometrics. *Diabetes, 58*(2), 453-459. doi:10.2337/db08-1112

Hashim, M., Radwan, H., Hasan, H., Obaid, R. S., Al Ghazal, H., Al Hilali, M., . . . Naja, F. (2019). Gestational weight gain and gestational diabetes among Emirati and Arab women in the United Arab Emirates: results from the MISC cohort. *BMC pregnancy and childbirth, 19*(1), 463. doi:10.1186/s12884-019-2621-z

Heslehurst, N., Vieira, R., Akhter, Z., Bailey, H., Slack, E., Ngongalah, L., . . . Rankin, J. (2019). The association between maternal body mass index and child obesity: A systematic review and meta-analysis. *PLOS Medicine, 16*(6), e1002817. doi:10.1371/journal.pmed.1002817

Holtrup, B., Church, C. D., Berry, R., Colman, L., Jeffery, E., Bober, J., & Rodeheffer, M. S. (2017). Puberty is an important developmental period for the establishment of adipose tissue mass and metabolic homeostasis. *Adipocyte, 6*(3), 224-233. doi:10.1080/21623945.2017.1349042

Hotamisligil, G. S., & Bernlohr, D. A. (2015). Metabolic functions of FABPs--mechanisms and therapeutic implications. *Nature reviews. Endocrinology, 11*(10), 592-605. doi:10.1038/nrendo.2015.122

Huang, P. L. (2009). A comprehensive definition for metabolic syndrome. *Disease models & mechanisms, 2*(5-6), 231-237. doi:10.1242/dmm.001180

Hudak, C. S., & Sul, H. S. (2013). Pref-1, a gatekeeper of adipogenesis. *Frontiers in endocrinology, 4*, 79. doi:10.3389/fendo.2013.00079

Hulme, C. H., Nicolaou, A., Murphy, S. A., Heazell, A. E. P., Myers, J. E., & Westwood, M. (2019). The effect of high glucose on lipid metabolism in the human placenta. *Scientific reports, 9*(1), 14114. doi:10.1038/s41598-019-50626-x

Isakson, P., Hammarstedt, A., Gustafson, B., & Smith, U. (2009). Impaired preadipocyte differentiation in human abdominal obesity: role of Wnt, tumor necrosis factor-alpha, and inflammation. *Diabetes, 58*(7), 1550-1557. doi:10.2337/db08-1770

Isomaa, B., Almgren, P., Tuomi, T., Forsén, B., Lahti, K., Nissén, M., . . . Groop, L. (2001). Cardiovascular Morbidity and Mortality Associated With the Metabolic Syndrome. *Diabetes Care, 24*(4), 683-689. doi:10.2337/diacare.24.4.683

Jeffery, E., Wing, A., Holtrup, B., Sebo, Z., Kaplan, Jennifer L., Saavedra-Peña, R., . . . Rodeheffer, Matthew S. (2016). The Adipose Tissue Microenvironment Regulates Depot-Specific Adipogenesis in Obesity. *Cell Metabolism, 24*(1), 142-150. doi:10.1016/j.cmet.2016.05.012

Jiang, Y., Berry, D. C., Tang, W., & Graff, J. M. (2014). Independent stem cell lineages regulate adipose organogenesis and adipose homeostasis. *Cell Rep, 9*(3), 1007-1022. doi:10.1016/j.celrep.2014.09.049

Kautzky-Willer, A., Pacini, G., Tura, A., Bieglmayer, C., Schneider, B., Ludvik, B., . . . Waldhäusl, W. (2001). Increased plasma leptin in gestational diabetes. *Diabetologia, 44*(2), 164-172. doi:10.1007/s001250051595

Kc, K., Shakya, S., & Zhang, H. (2015). Gestational Diabetes Mellitus and Macrosomia: A Literature Review. *Annals of Nutrition and Metabolism, 66*(Suppl. 2), 14-20. doi:10.1159/000371628

Kenna, L. A., Olsen, J. A., Spelios, M. G., Radin, M. S., & Akirav, E. M. (2016). β-Cell death is decreased in women with gestational diabetes mellitus. *Diabetology & metabolic syndrome, 8*(1), 60. doi:10.1186/s13098-016-0175-z

Kirwan, J. P., Varastehpour, A., Jing, M., Presley, L., Shao, J., Friedman, J. E., & Catalano, P. M. (2004). Reversal of Insulin Resistance Postpartum Is Linked to Enhanced Skeletal Muscle Insulin Signaling. *The Journal of Clinical Endocrinology & Metabolism, 89*(9), 4678-4684. doi:10.1210/jc.2004-0749

Klok, M. D., Jakobsdottir, S., & Drent, M. L. (2007). The role of leptin and ghrelin in the regulation of food intake and body weight in humans: a review. *Obesity Reviews, 8*(1), 21-34. doi:10.1111/j.1467-789X.2006.00270.x

Kwok, K. H. M., Lam, K. S. L., & Xu, A. (2016). Heterogeneity of white adipose tissue: molecular basis and clinical implications. *Experimental & molecular medicine, 48*(3), e215-e215. doi:10.1038/emm.2016.5

Lavery, J. A., Friedman, A. M., Keyes, K. M., Wright, J. D., & Ananth, C. V. (2017). Gestational diabetes in the United States: temporal changes in prevalence rates between 1979 and 2010. *BJOG : an international journal of obstetrics and gynaecology, 124*(5), 804-813. doi:10.1111/1471-0528.14236

Lee, M.-W., Lee, M., & Oh, K.-J. (2019). Adipose Tissue-Derived Signatures for Obesity and Type 2 Diabetes: Adipokines, Batokines and MicroRNAs. *Journal of clinical medicine, 8*(6), 854. doi:10.3390/jcm8060854

Liu, T., Fang, Z., Yang, D., & Liu, Q. (2012). [Correlation between the inflammatory factors and adipocytokines with gestational diabetes mellitus and their change in puerperium]. *Zhonghua Fu Chan Ke Za Zhi, 47*(6), 436-439.

Lobstein, T., & Jackson-Leach, R. (2016). Planning for the worst: estimates of obesity and comorbidities in school-age children in 2025. *Pediatric Obesity, 11*(5), 321-325. doi:10.1111/ijpo.12185

Longo, M., Zatterale, F., Naderi, J., Parrillo, L., Formisano, P., Raciti, G. A., . . . Miele, C. (2019). Adipose Tissue Dysfunction as Determinant of Obesity-Associated Metabolic Complications. *International journal of molecular sciences, 20*(9), 2358. doi:10.3390/ijms20092358

Madsen, M. S., Siersbæk, R., Boergesen, M., Nielsen, R., & Mandrup, S. (2014). Peroxisome proliferator-activated receptor γ and C/EBPα synergistically activate key metabolic adipocyte genes by assisted loading. *Molecular and Cellular Biology, 34*(6), 939-954. doi:10.1128/MCB.01344-13

Majka, S. M., Barak, Y., & Klemm, D. J. (2011). Concise review: adipocyte origins: weighing the possibilities. *Stem cells (Dayton, Ohio), 29*(7), 1034-1040. doi:10.1002/stem.653

Marciniak, A., Patro-Małysza, J., Kimber-Trojnar, Ż., Marciniak, B., Oleszczuk, J., & Leszczyńska-Gorzelak, B. (2017). Fetal programming of the metabolic syndrome. *Taiwanese Journal of Obstetrics and Gynecology*, *56*(2), 133-138. doi:https://doi.org/10.1016/j.tjog.2017.01.001

Marco, L. J., McCloskey, K., Vuillermin, P. J., Burgner, D., Said, J., & Ponsonby, A.-L. (2012). Cardiovascular Disease Risk in the Offspring of Diabetic Women: The Impact of the Intrauterine Environment. *Experimental Diabetes Research, 2012*, 565160. doi:10.1155/2012/565160

Mirghani, H., Zayed, R., Thomas, L., & Agarwal, M. (2007). Gestational diabetes mellitus: fetal liver length measurements between 21and 24 weeks' gestation. *J Clin Ultrasound, 35*(1), 34-37. doi:10.1002/jcu.20294

Mlinar, B., & Marc, J. (2011). New insights into adipose tissue dysfunction in insulin resistance. *Clinical Chemistry and Laboratory Medicine (CCLM), 49*(12), 1925-1935. doi:https://doi.org/10.1515/CCLM.2011.697

Moseti, D., Regassa, A., & Kim, W.-K. (2016). Molecular Regulation of Adipogenesis and Potential Anti-Adipogenic Bioactive Molecules. *International journal of molecular sciences, 17*(1), 124. doi:10.3390/ijms17010124

Müller, M. J., & Geisler, C. (2017). Defining obesity as a disease. *European Journal of Clinical Nutrition, 71*(11), 1256-1258. doi:10.1038/ejcn.2017.155

Myers, M. G., Jr., Heymsfield, S. B., Haft, C., Kahn, B. B., Laughlin, M., Leibel, R. L., . . . Yanovski, J. A. (2012). Challenges and opportunities of defining clinical leptin resistance. *Cell Metab, 15*(2), 150-156. doi:10.1016/j.cmet.2012.01.002

Nadeau, K. J., Maahs, D. M., Daniels, S. R., & Eckel, R. H. (2011). Childhood obesity and cardiovascular disease: links and prevention strategies. *Nature reviews. Cardiology, 8*(9), 513-525. doi:10.1038/nrcardio.2011.86

Nakae, J., Kitamura, T., Kitamura, Y., Biggs, W. H., III, Arden, K. C., & Accili, D. (2003). The Forkhead Transcription Factor Foxo1 Regulates Adipocyte Differentiation. *Developmental Cell, 4*(1), 119-129. doi:10.1016/S1534-5807(02)00401-X

Nieva-Vazquez, A., Pérez-Fuentes, R., Torres-Rasgado, E., López-López, J. G., & Romero, J. R. (2014). Serum resistin levels are associated with adiposity and insulin sensitivity in obese Hispanic subjects. *Metabolic syndrome and related disorders, 12*(2), 143-148. doi:10.1089/met.2013.0118

Norata, G. D., Ongari, M., Garlaschelli, K., Raselli, S., Grigore, L., & Catapano, A. L. (2007). Plasma resistin levels correlate with determinants of the metabolic syndrome. *Eur J Endocrinol, 156*(2), 279-284. doi:10.1530/eje.1.02338

Olmos, P. R., Rigotti, A., Busso, D., Berkowitz, L., Santos, J. L., Borzone, G. R., . . . Mertens, N. (2014). Maternal hypertriglyceridemia: A link between maternal overweight-obesity and macrosomia in gestational diabetes. *Obesity, 22*(10), 2156-2163. doi:10.1002/oby.20816

Otto, T. C., & Lane, M. D. (2005). Adipose Development: From Stem Cell to Adipocyte. *Critical Reviews in Biochemistry and Molecular Biology, 40*(4), 229-242. doi:10.1080/10409230591008189

Ovesen, P. G., Fuglsang, J., Andersen, M. B., Wolff, C., Petersen, O. B., & David McIntyre, H. (2018). Temporal Trends in Gestational Diabetes Prevalence, Treatment, and Outcomes at Aarhus University Hospital, Skejby, between 2004 and 2016. *Journal of diabetes research, 2018,* 5937059. doi:10.1155/2018/5937059

Parameswaran, N., & Patial, S. (2010). Tumor necrosis factor-α signaling in macrophages. *Critical reviews in eukaryotic gene expression, 20*(2), 87-103. doi:10.1615/critreveukargeneexpr.v20.i2.10

Park, H. K., Kwak, M. K., Kim, H. J., & Ahima, R. S. (2017). Linking resistin, inflammation, and cardiometabolic diseases. *The Korean journal of internal medicine, 32*(2), 239-247. doi:10.3904/kjim.2016.229

Park, Y.-M., Myers, M., & Vieira-Potter, V. J. (2014). Adipose tissue inflammation and metabolic dysfunction: role of exercise. *Missouri medicine, 111*(1), 65-72. Retrieved from https://www.ncbi.nlm.nih.gov/pmc/articles/PMC6179510/

Payne, V. A., Au, W.-S., Lowe, C. E., Rahman, S. M., Friedman, J. E., O'Rahilly, S., & Rochford, J. J. (2009). C/EBP transcription factors regulate SREBP1c gene expression during adipogenesis. *The Biochemical journal, 425*(1), 215-223. doi:10.1042/BJ20091112

Pereira, T. J., Fonseca, M. A., McGavock, J. M., & Dolinsky, V. W. (2013). Early Life Development of Cardiac Hypertrophy in Rat Offspring from Pregnancies Complicated by

Gestational Diabetes Mellitus. *Canadian Journal of Diabetes, 37*, S63-S64. doi:10.1016/j.jcjd.2013.08.192

Perng, W., Rifas-Shiman, S. L., McCulloch, S., Chatzi, L., Mantzoros, C., Hivert, M. F., & Oken, E. (2017). Associations of cord blood metabolites with perinatal characteristics, newborn anthropometry, and cord blood hormones in project viva. *Metabolism, 76*, 11-22. doi:10.1016/j.metabol.2017.07.001

Pilz, S., & März, W. (2008). Free fatty acids as a cardiovascular risk factor. *Clinical Chemistry and Laboratory Medicine (CCLM), 46*(4), 429-434. doi:https://doi.org/10.1515/CCLM.2008.118

Raitakari, O. T., Juonala, M., Kähönen, M., Taittonen, L., Laitinen, T., Mäki-Torkko, N., . . . Viikari, J. S. A. (2003). Cardiovascular Risk Factors in Childhood and Carotid Artery Intima-Media Thickness in Adulthood: The Cardiovascular Risk in Young Finns Study. *JAMA, 290*(17), 2277-2283. doi:10.1001/jama.290.17.2277

Roseboom, T. J. (2019). Epidemiological evidence for the developmental origins of health and disease: effects of prenatal undernutrition in humans. *J Endocrinol, 242*(1), T135-t144. doi:10.1530/joe-18-0683

Ryckman, K., Spracklen, C., Smith, C., Robinson, J., & Saftlas, A. (2015). Maternal lipid levels during pregnancy and gestational diabetes: a systematic review and meta-analysis. *BJOG: An International Journal of Obstetrics & Gynaecology, 122*(5), 643-651. doi:10.1111/1471-0528.13261

Ryckman, K. K., Borowski, K. S., Parikh, N. I., & Saftlas, A. F. (2013). Pregnancy Complications and the Risk of Metabolic Syndrome for the Offspring. *Current cardiovascular risk reports, 7*(3), 217-223. doi:10.1007/s12170-013-0308-y

Sacks, D. A., Hadden, D. R., Maresh, M., Deerochanawong, C., Dyer, A. R., Metzger, B. E., . . . Trimble, E. R. (2012). Frequency of Gestational Diabetes Mellitus at Collaborating Centers Based on IADPSG Consensus Panel–Recommended Criteria. *The Hyperglycemia and Adverse Pregnancy Outcome (HAPO) Study, 35*(3), 526-528. doi:10.2337/dc11-1641

Sánchez-Solana, B., Laborda, J., & Baladrón, V. (2012). Mouse resistin modulates adipogenesis and glucose uptake in 3T3-L1 preadipocytes through the ROR1 receptor. *Molecular endocrinology (Baltimore, Md.), 26*(1), 110-127. doi:10.1210/me.2011-1027

Saponaro, C., Gaggini, M., Carli, F., & Gastaldelli, A. (2015). The Subtle Balance between Lipolysis and Lipogenesis: A Critical Point in Metabolic Homeostasis. *Nutrients, 7*(11), 9453-9474. doi:10.3390/nu7115475

Schwartz, M. W., Woods, S. C., Seeley, R. J., Barsh, G. S., Baskin, D. G., & Leibel, R. L. (2003). Is the Energy Homeostasis System Inherently Biased Toward Weight Gain? *Diabetes, 52*(2), 232-238. doi:10.2337/diabetes.52.2.232

Shanik, M. H., Xu, Y., Škrha, J., Dankner, R., Zick, Y., & Roth, J. (2008). Insulin Resistance and Hyperinsulinemia. *Is hyperinsulinemia the cart or the horse?, 31*(Supplement 2), S262-S268. doi:10.2337/dc08-s264

Singh, G. K., & DiBari, J. N. (2019). Marked Disparities in Pre-Pregnancy Obesity and Overweight Prevalence among US Women by Race/Ethnicity, Nativity/Immigrant Status, and Sociodemographic Characteristics, 2012–2014. *Journal of Obesity, 2019*, 2419263. doi:10.1155/2019/2419263

Steffensen, K. R., & Gustafsson, J.-Å. (2004). Putative Metabolic Effects of the Liver X Receptor (LXR). *Diabetes, 53*(suppl 1), S36-S42. doi:10.2337/diabetes.53.2007.S36

Stubbins, R. E., Najjar, K., Holcomb, V. B., Hong, J., & Núñez, N. P. (2012). Oestrogen alters adipocyte biology and protects female mice from adipocyte inflammation and insulin resistance. *Diabetes, obesity & metabolism, 14*(1), 58-66. doi:10.1111/j.1463-1326.2011.01488.x

Sun, K., Tordjman, J., Clément, K., & Scherer, Philipp E. (2013). Fibrosis and Adipose Tissue Dysfunction. *Cell Metabolism, 18*(4), 470-477. doi:10.1016/j.cmet.2013.06.016

Tang, Q.-Q., Otto, T. C., & Lane, M. D. (2003). Mitotic clonal expansion: A synchronous process required for adipogenesis. *Proceedings of the National Academy of Sciences, 100*(1), 44-49. doi:10.1073/pnas.0137044100

Tang, W., Zeve, D., Suh, J. M., Bosnakovski, D., Kyba, M., Hammer, R. E., . . . Graff, J. M. (2008). White fat progenitor cells reside in the adipose vasculature. *Science, 322*(5901), 583-586. doi:10.1126/science.1156232

Tchoukalova, Y., Koutsari, C., & Jensen, M. (2007). Committed subcutaneous preadipocytes are reduced in human obesity. *Diabetologia, 50*(1), 151-157. doi:10.1007/s00125-006-0496-9

Toth, P. P. (2016). Triglyceride-rich lipoproteins as a causal factor for cardiovascular disease. *Vascular health and risk management, 12*, 171-183. doi:10.2147/VHRM.S104369

Tran, T. T., Yamamoto, Y., Gesta, S., & Kahn, C. R. (2008). Beneficial effects of subcutaneous fat transplantation on metabolism. *Cell Metabolism, 7*(5), 410-420. doi:10.1016/j.cmet.2008.04.004

Urrutia, O., Alfonso, L., & Mendizabal, J. A. (2018). Cellularity Description of Adipose Depots in Domesticated Animals. In L. Szablewski (Ed.), *Adipose Tissue* (pp. 73-90). doi:10.5772/intechopen.74109

Virtue, S., & Vidal-Puig, A. (2010). Adipose tissue expandability, lipotoxicity and the Metabolic Syndrome — An allostatic perspective. *Biochimica et Biophysica Acta (BBA) - Molecular and Cell Biology of Lipids, 1801*(3), 338-349. doi:https://doi.org/10.1016/j.bbalip.2009.12.006

Wang, Q. A., Tao, C., Gupta, R. K., & Scherer, P. E. (2013). Tracking adipogenesis during white adipose tissue development, expansion and regeneration. *Nature Medicine, 19*(10), 1338-1344. doi:10.1038/nm.3324

Wei, S., Zhang, L., Zhou, X., Du, M., Jiang, Z., Hausman, G. J., . . . Dodson, M. V. (2013). Emerging roles of zinc finger proteins in regulating adipogenesis. *Cellular and molecular life sciences : CMLS, 70*(23), 4569-4584. doi:10.1007/s00018-013-1395-0

Wilcox, G. (2005). Insulin and insulin resistance. *The Clinical biochemist. Reviews, 26*(2), 19-39. Retrieved from https://pubmed.ncbi.nlm.nih.gov/16278749

Zhang, K.-M., Tu, K., Li, Y.-X., Zhu, L., Xiao, H.-S., Yang, Y., & Wu, J.-R. (2009). Adipogenesis licensing and execution are disparately linked to cell proliferation. *Cell research, 19*, 216-223. doi:10.1038/cr.2008.319

Zomer, H. D., Vidane, A. S., Gonçalves, N. N., & Ambrósio, C. E. (2015). Mesenchymal and induced pluripotent stem cells: general insights and clinical perspectives. *Stem cells and cloning : advances and applications, 8*, 125-134. doi:10.2147/SCCAA.S88036